

1 Acclimation of *Chlamydomonas reinhardtii* to
2 extremely strong light

3

4 Olli Virtanen, Sergey Khorobrykh and Esa Tyystjärvi *

5 *University of Turku, Department of Biochemistry / Molecular Plant Biology, FI-20014 Turku, Finland*

6 *Corresponding author, email: esatyy@utu.fi

7 ORCID IDs: OV (0000-0002-2991-520X), SK (0000-0002-0153-5133), ET (0000-0001-6808-7470)

8

9

10

11

12

13

14

15

16

17

18 Acknowledgements

19

20 This study was financially supported by Academy of Finland (grants 307335 and 333421),

21 University of Turku Graduate School (UTUGS) and NordForsk (NordAqua project).

22 Abstract

23

24 Most photosynthetic organisms are sensitive to very high light, although acclimation
25 mechanisms enable them to deal with exposure to strong light up to a point. Here we show that
26 cultures of wild-type *Chlamydomonas reinhardtii* strain *cc124*, when exposed to
27 photosynthetic photon flux density $3000 \mu\text{mol m}^{-2} \text{s}^{-1}$ for a couple of days, are able to suddenly
28 attain the ability to grow and thrive. We compared the phenotypes of control cells and cells
29 acclimated to this extreme light (EL). The results suggest that genetic or epigenetic variation,
30 developing during maintenance of the population in moderate light, contributes to the
31 acclimation capability. EL acclimation was associated with a high carotenoid-to-chlorophyll
32 ratio and slowed down PSII charge recombination reactions, probably by affecting the pre-
33 exponential Arrhenius factor of the rate constant. In agreement with these findings, EL
34 acclimated cells showed only one tenth of the $^1\text{O}_2$ level of control cells. In spite of low $^1\text{O}_2$
35 levels, the rate of the damaging reaction of PSII photoinhibition was similar in EL acclimated
36 and control cells. Furthermore, EL acclimation was associated with slow PSII electron transfer
37 to artificial quinone acceptors. The data show that ability to grow and thrive in extremely strong
38 light is not restricted to photoinhibition-resistant organisms such as *Chlorella ohadii* or to high-
39 light tolerant mutants, but a wild-type strain of a common model microalga has this ability as
40 well.

41

42 Keywords: *Chlamydomonas reinhardtii* • Photosystem II • PSII • high light • extreme light •
43 acclimation • light stress

44 Declarations

45

46 Funding

47 This study was financially supported by Academy of Finland (grants 307335 and 333421),
48 NordForsk (NordAqua project) and University of Turku Graduate School (UTUGS).

49 Conflicts of interest/Competing interests

50 The authors declare that they have no conflict of interest.

51 Ethics approval

52 Not applicable

53 Consent to participate

54 Not applicable

55 Consent for publication

56 Not applicable

57 Availability of data and material

58 A dataset is available at [https://data.mendeley.com/datasets/fwnzkph5w2/draft?a=bd44a7ec-
59 58544a-4e7b-9043-f773adf5065b](https://data.mendeley.com/datasets/fwnzkph5w2/draft?a=bd44a7ec-58544a-4e7b-9043-f773adf5065b)

60 Code availability

61 Not applicable

62 Author's contributions

63 OV did all of the laboratory work unless otherwise stated and composed the manuscript. SK
64 analyzed the data generated related to plastoquinone experiments. ET supervised the work,
65 oversaw the study from plan to completion and was a major contributor in writing the
66 manuscript. All authors read and approved the final version of the manuscript.

67 Introduction

68 Light is the driving force of photosynthesis but also a stress factor affecting both photosystems.
69 Photosystem II (PSII) is particularly susceptible to light-induced damage, and the rate of
70 damage is proportional to light intensity (Tyystjärvi and Aro 1996). Photoinhibition is
71 counteracted by concurrent repair, and several biochemical mechanisms offer partial protection
72 (for review, see Tyystjärvi 2013), but in spite of the protective mechanisms, light intensities
73 far above saturation are expected to lower the number of active PSII units and thereby cause
74 decrease in the photosynthetic rate. Furthermore, reactive oxygen species produced in very
75 high light are also expected to cause oxidative damage, and oxidative repression of translational
76 elongation (Nishiyama et al. 2004) directly interfering with the repair of photoinhibitory
77 damage.

78 Green microalgae that live in surface waters are exposed to periods of high light. Earlier
79 experiments have shown that *C. reinhardtii*, when exposed to strong light for some time, can
80 form cultures that can be continuously grown in strong light (Förster et al. 2005). Mutation
81 leading to a high-light tolerant phenotype is an obvious possible mechanism for these changes,
82 and high-light tolerant mutants of *C. reinhardtii* have been isolated (Förster et al. 2005;
83 Schierenbeck et al. 2015), and at least the high-light tolerant *hit2*-mutant has properties that
84 enables it to tolerate photoinhibition of PSII (Virtanen et al. 2019). We exposed the wild-type
85 strain *cc124* of *C. reinhardtii* to extremely strong light (EL) and found that the alga regularly
86 switches to a phenotype tolerant to EL after only a few days of exposure to EL conditions. The
87 change is too rapid and frequent to be caused by random mutations, which prompted us to
88 explore acclimatory changes in photoprotective mechanisms.

89 Studies of both damage and acclimation to high light have largely focused on PSII because
90 PSII is much more sensitive to high light than PSI in strong continuous light (Tyystjärvi et al.

91 1989; Sonoike 1996), PSII is the major producer of the harmful singlet oxygen ($^1\text{O}_2$) in
92 photosynthetic organisms (Hideg and Vass 1995; Fufezan et al. 2002; Krieger-Liszkay 2005;
93 Krieger-Liszkay et al. 2008; Cazzaniga et al. 2012; Telfer 2014, for recent review on singlet
94 oxygen see Dimitrieva et al. 2020), and because the rapid turnover of the D1 protein in high
95 light makes PSII specifically sensitive to damage to the translation machinery (Nishiyama et
96 al. 2001; Nishiyama et al. 2004). The short lifetimes of excited chlorophylls in PSI (for review,
97 see Chukhutsina et al. 2019) do not favor production of $^1\text{O}_2$ in PSI antenna. Instead of
98 producing $^1\text{O}_2$, PSI can reduce oxygen to superoxide in Mehler's reaction (Lima-Melo et al.
99 2019). Reactive oxygen species are linked to inactivation of PSI (for review, see Sonoike 2011;
100 for their importance in fluctuating light see Sejima et al. 2014) but in high light, the primary
101 donor of PSI tends to stay oxidized, which protects PSI against damage (for review, see
102 Shimakawa and Miyake 2018). Furthermore, as Mehler's reaction and inactivation of PSI
103 require PSII electron transfer, inactivation of PSI is not directly dependent on light. Moreover,
104 PSI is also protected by several different mechanisms regulating electron transfer (for review,
105 see Tikkanen and Aro 2014) and by down-regulation of PSII in high light (Ivanov et al. 1998;
106 Lima-Melo et al. 2019). For these reasons, our focus will be on PSII, although we cannot rule
107 out additional acclimation responses that might specifically protect other parts of the
108 photosynthetic machinery, especially PSI, during exposure to EL.

109 Non-photochemical quenching of absorbed excitation energy (NPQ) is a major PSII-specific
110 mechanism that helps to avoid the damage caused by high light (Wobbe et al 2016). However,
111 NPQ mechanisms protect the system only up to a degree (Sarvikas et al. 2006; Havurinne et
112 al. 2019). In contrast to plants, where the most rapidly induced component of NPQ is ΔpH
113 dependent heat dissipation (qE), the most rapid response to high light in green algae is a state
114 transition leading to qT-type NPQ. Light-Harvesting Complex Stress-Related proteins 1 and 3
115 (LHCSR) are constitutively present in *C. reinhardtii* cells grown in the light (Nawrocki et al.

116 2019), and they are activated by light-induced decrease in lumenal pH (Bonente et al. 2011;
117 Liguori et al. 2013; Kondo et al. 2017; Tian et al. 2019). Active LHCSR3 induces rapid
118 decoupling of LHCII from PSII shortly after the beginning of high-light exposure (Roach and
119 Na 2017). Chlorophylls (Chls) of decoupled LHCII have a very short excitation lifetime and
120 function as excitation energy sinks (Ünlü et al. 2014). The decoupling also efficiently decreases
121 the functional antenna size of PSII (Tian et al. 2019). These mechanisms are considered to
122 protect the system efficiently although the LHCSRs are also required for the formation of qE
123 within several hours of high-light exposure (Peers et al. 2009; Allorent et al. 2013).
124 Furthermore, acidification of the thylakoid lumen activates the STT7 kinase that
125 phosphorylates LHCII that then decouples from PSII and moves to serve PSI like in higher
126 plants. In *C. reinhardtii*, 80 % of LHCII can disassociate from PSII (Delosme et al. 1996) while
127 only 15 % is estimated to move between photosystems in *A. thaliana* (Allen 1992). However,
128 in *C. reinhardtii* only a small part of LHCII that is decoupled from PSII transfers excitation
129 energy to PSI (Nagy et al. 2014; Ünlü et al. 2014), further emphasizing the photoprotective
130 role of qT in *C. reinhardtii*. In addition to the LHCSR-dependent excitation energy quenching,
131 *C. reinhardtii* down-regulates the amount of Chl per cell and up-regulates the carotenoid-to-
132 Chl ratio upon long exposure to high light (Virtanen et al. 2019). These mechanisms decrease
133 the incoming excitation of PSII and promote quenching of reactive oxygen species by
134 carotenoids. In addition, the PSI to PSII ratio is down-regulated during acclimation to high
135 light in *C. reinhardtii*; the advantage of this response, however, is not known (Bonente et al.
136 2012; Virtanen et al. 2019).

137 Generally, high-light-tolerating or slow-photoinhibition phenotypes produced by mutations are
138 relatively mild. For example, at the photosynthetic photon flux density (PPFD) of 1250 μmol
139 $\text{m}^{-2} \text{s}^{-1}$, the continuous productivity of the high-light tolerant *hit2* mutant of *C. reinhardtii*
140 (Schierenbeck et al. 2015) with a mutation in the *Cr-COPI* gene involved in ultraviolet

141 signaling (Tilbrook et al. 2016), is only one fourth higher than that of the wild type (Virtanen
142 et al. 2019). In addition, the redox potential of the Q_A/Q_A^- pair determines the probability of
143 formation of a triplet state of the primary donor by PSII recombination reactions, thereby
144 affecting the probability of formation of the poisonous singlet oxygen (1O_2) (Krieger-Liszkay
145 et al. 2008). In the cyanobacterium *Synechococcus elongatus*, the A249S mutation of the D1
146 protein makes the redox potential of the Q_A/Q_A^- pair more positive and causes a lowering of
147 approximately one fourth in the rate of photoinhibition compared to the wild type (Fufezan et
148 al. 2007). Because the rate constant of photoinhibition is directly proportional to light intensity
149 (Tyystjärvi and Aro 1996), protection by one fourth suggests that the mutants would tolerate
150 approximately one fourth higher light intensity than the wild type.

151 In the present study, we show that wild-type cells of *C. reinhardtii* regularly develop a
152 capability to grow rapidly at PPFD $3000 \mu\text{mol m}^{-2} \text{s}^{-1}$ in mineral medium. This PPFD is
153 approximately 1.5 times full sunlight and 10-20 times as high as usually applied in laboratory
154 cultivation of *C. reinhardtii*. Photosynthetic properties and 1O_2 production of cells growing in
155 this extremely strong light were compared to those growing at moderate PPFD to pinpoint the
156 features that might cause the observed tolerance.

157

158 Materials and methods

159

160 Algal strain and growth conditions

161

162 All experiments were conducted with the *cc124* wild-type strain of *C. reinhardtii*. The cells
163 were maintained on Tris-Acetate-Phosphate (TAP) plates (Gorman and Levine 1965) and

164 transferred to a liquid, photoautotrophic high salt (HS) medium (Sueoka 1960) prior to the
165 experiments. In this liquid HS-medium, the cells were first kept in pre-culture conditions in
166 moderate light conditions (27 °C, PPFD 100 $\mu\text{mol m}^{-2} \text{s}^{-1}$) to acclimate the cells to
167 photoautotrophy. The cells were grown in 1 % CO_2 to enhance photosynthetic growth during
168 this precultivation.

169

170 Extreme-light growth experiment

171

172 Experiments testing the ability of the cells to grow in extremely strong light were done by
173 cultivating two types of cultures in these conditions. Two types of cultures prepared for
174 growing in extreme light conditions were isolated subpopulations that were populations
175 inoculated from the original culture, and populations originating from single, individual cells
176 of the original culture obtained via dilution and plating on solid HS medium. These isolated
177 subpopulations or single-cell-originating cultures of *cc124*, as indicated, were then first
178 cultivated in liquid HS medium in pre-culture conditions (27 °C, PPFD 100 $\mu\text{mol m}^{-2} \text{s}^{-1}$, 1 %
179 CO_2) and then diluted to OD_{730} (optical density at 730 nm) of 0.01. The diluted 45 ml cultures
180 in HS medium were transferred to PPFD 3000 $\mu\text{mol m}^{-2} \text{s}^{-1}$, 26 °C and ambient air (hereafter
181 referred to as extreme light, EL) in 100 ml Erlenmeyer flasks. Mixing was provided with an
182 orbital shaker. Combination of white 30 W LEDs (LED Energie, Model no. 6208 5667)) and
183 10 W LEDs (IKEA, Product no. LED1506R10) were used to create the extremely strong light
184 (see Fig. S1 for the illumination spectrum in the EL conditions). Growth was monitored for 96
185 hours by daily measurements of OD_{730} , and cultures whose OD_{730} had increased to 0.05 were
186 used for further experiments. The EL experiment was conducted with 30 biological replicates
187 of both isolated subpopulation and single cell types of inocula.

188

189 Pigment concentrations

190

191 Samples for pigment extraction were taken from cultures diluted to OD_{730} of 0.5. 1 ml aliquots
192 were centrifuged for 10 min at $14\,000\times g$ and resuspended in 1 ml of methanol. After thorough
193 mixing, the pigments were extracted in cold ($+4^{\circ}C$) and darkness. After 24 h of extraction, the
194 samples were centrifuged for 10 min at $14\,000\times g$, after which absorbance of the supernatant
195 was measured at 470, 652.4 and 665.2 nm, and the pigments were quantified according to
196 Wellburn (1994).

197

198 Low temperature fluorescence spectra

199

200 The samples for fluorescence emission were taken directly from EL and control cultures and
201 stored at $-80^{\circ}C$ until measured. The samples were diluted to the Chl concentration of $1.5\ \mu g$
202 $Chl\ ml^{-1}$ and a final volume of $50\ \mu l$ just prior to the measuring the spectra *in vivo*. Frozen
203 samples were illuminated at liquid nitrogen temperature ($-196^{\circ}C$) with 442 nm blue light, and
204 fluorescence emission was measured with a QEPro spectrometer (Ocean Insight, Ostfildern,
205 Germany).

206

207 Plastoquinone measurement

208

209 The total amount of plastoquinone (PQ) was determined from EL and control cells with high
210 performance liquid chromatography (Khorobrykh et al. 2020) by utilizing the detection of
211 fluorescence of reduced plastoquinone (PQH₂) at 330 nm with excitation wavelength at
212 290 nm. The preparation of the calibration standard has been published earlier (Khorobrykh et
213 al. 2020). Quantities obtained were then normalized to the Chl concentrations, measured
214 separately from all three biological replicates.

215

216 Quantification of PSII and PSI

217

218 Proteins were extracted from approximately 20 million cells, collected via centrifugation (12
219 000 × g, 10 min) and resuspended in protein extraction buffer (50 mM Tris-HCl; pH = 8, 2 %
220 SDS, 10 mM EDTA). After resuspension, the cells were frozen in liquid nitrogen, followed by
221 thawing in a 45 °C water bath. This was repeated three times in rapid succession, after which
222 the debris was removed via centrifugation (15 000 × g, 5 min).

223 The relative amounts of PSII and PSI were estimated from Western blots with antibodies for
224 two of their core proteins, CP43 and PsaA, respectively. Proteins were first separated with
225 SDS-PAGE, using 1 µg (for CP43) or 2 µg (for PsaA) of protein per well. These amounts of
226 protein were found to be optimal for detection through dilution series. Primary antibodies for
227 CP43 (Agrisera, Product No. AS06 110) and PsaA (Agrisera, Product No. AS06 172) were
228 used in concentrations of 1:6000 and 1:5000, respectively. The secondary antibody, goat-anti
229 rabbit IgG (H+L), alkaline phosphatase conjugate (Life technologies, REF G21079) was used
230 in final concentration of 1:50 000 and the binding was detected via luminescence caused by
231 alkaline phosphatase. Relative amounts of the proteins were calculated from signal intensities,
232 quantified with the image processing software Fiji (Fiji Is Just ImageJ, v. 1.52).

233

234 Oxygen evolution measurements

235

236 The light-saturated rate of oxygen evolution (under PPFD 2000 $\mu\text{mol m}^{-2} \text{s}^{-1}$) was measured
237 from 1 ml samples of intact cells with a Clark-type oxygen electrode (Hansatech Instruments
238 Ltd, Norfolk, United Kingdom) at 25 °C in HS medium. For comparison of electron acceptors,
239 the samples were diluted to OD_{730} of 0.5. Artificial electron acceptor 2,6-
240 dimethylbenzoquinone (DMBQ, 0.5 mM); 2,5-dichloro-1,4-benzoquinone (DCBQ, 0.5 mM);
241 ferricyanide (FeCy, 0.5 mM), or an inhibitor of electron transfer (2,5-dibromo-6-isopropyl-3-
242 methyl-1,4-benzoquinone (DBMIB, 0.5 μM), as indicated, was added just before the
243 measurement.

244 Thylakoids were isolated as described previously in Virtanen et al. 2019. The chlorophyll
245 concentration of the thylakoid isolates was determined spectrophotometrically according to
246 Porra et al. 1989. Isolated thylakoids were stored at -70 °C till measurements. Oxygen evolution
247 of the isolated thylakoids was measured as *in vivo* except that thylakoids were diluted in PSII
248 measuring buffer (40 mM HEPES-KOH pH 7.6; 0.33 M sorbitol; 5 mM MgCl_2 ; 5 mM NaCl;
249 1 M glycine betaine; 1 mM KH_2PO_4 ; 5 mM NH_2Cl) in final volume of 1 ml and chlorophyll
250 concentration of 5 $\mu\text{g ml}^{-1}$. DMBQ, DCBQ and FeCy were applied in the same concentrations
251 as used for the *in vivo*-measurements.

252

253 Fluorescence measurements

254

255 Chl *a* fluorescence decay after a single turnover flash (60 % of maximum voltage
256 corresponding to PPFD $10^5 \mu\text{mol m}^{-2} \text{s}^{-1}$, as reported by manufacturer, flash duration 30 μs)
257 was measured with a Superhead high-sensitivity detector, connected to an FL200/PS control
258 unit (Photon Systems Instruments, Drásov, Czech Republic) from 2 ml samples with $5 \mu\text{g ml}^{-1}$
259 of Chl at 25 °C in the presence and absence of 10 μM 3-(3,4-dichlorophenyl)-1,1-
260 dimethylurea (DCMU), as indicated. Before measurement, the samples were dark-incubated
261 for 15 min in ambient air. Each measurement lasted for 120 seconds, the first data point was
262 recorded 300 μs after the single turnover flash, and three independent biological replicates were
263 measured for all conditions. Results in the presence of DCMU were fitted to a first-order
264 reaction to obtain the rate constant of recombination reactions. *Copasi*-software (Hoops et al.
265 2006) was used for fitting.

266 Fluorescence induction was measured both in the absence and in the presence of 10 μM DCMU
267 from intact *C. reinhardtii* cells with AquaPen fluorometer (AquaPen AP100, Photon Systems
268 Instruments, Drásov, Czech Republic). 2 ml samples with Chl concentration of $1 \mu\text{g ml}^{-1}$ were
269 dark-incubated for 15 min in ambient air, and the intensity of the actinic light was set to 40 %
270 of the maximum of the instrument. Actinic light intensity and Chl concentration were
271 optimized in preliminary experiments to obtain a valid signal. DCMU, when used, was added
272 before the 15 min dark-incubation in the final concentration of 10 μM . Three independent
273 biological replicates were measured from all conditions.

274

275 Thermoluminescence

276

277 Thermoluminescence was measured *in vivo* with an apparatus described before (Tyystjärvi et
278 al. 2009) from 200 μl samples containing 3.1 μg Chl. For Q band measurements, 10 μM DCMU

279 was added. The samples were dark-incubated at 20 °C for 5 min and then cooled to either -10
280 °C for B band measurement or -20 °C for Q band measurement, as indicated. The frozen sample
281 was charged with a single turnover flash ($E=1$ J) from a Xenon flash lamp and photon emission
282 was recorded during warming to 60 °C with a heating rate of 0.66 °C s⁻¹. Simulation of
283 thermoluminescence was done with the *Copasi* software. In the simulation,
284 thermoluminescence intensity during heating from 274 to 340 K with the rate of 0.66 K s⁻¹ was
285 simulated as the rate of a first-order reaction whose rate constant is $s \times \exp(-501 \text{ meV}/(k_b \times$
286 $(274 \text{ K} + 0.66 \text{ K s}^{-1} \times t))$, where s is a pre-exponential factor, k_b is Boltzmann's constant, β is
287 the heating rate and t is time from start of heating. 501 meV is the activation energy.

288

289 Singlet oxygen production

290

291 ¹O₂ production by *C. reinhardtii* was measured *in vivo* by using Singlet Oxygen Sensor Green
292 (SOSG) (Invitrogen by ThermoFischer Scientific). Cell cultures were concentrated through
293 gentle centrifugation (100 × g, 1 min) to a Chl concentration of 50 µg ml⁻¹. SOSG was added
294 to 350 µl samples in final concentration of 50 µM. ¹O₂ production was induced by illuminating
295 the samples with red light, PPFD 2000 µmol m⁻² s⁻¹, obtained from a slide projector and a 650
296 nm long-pass filter (Corion LL650, Newport Corp.). SOSG fluorescence was recorded every
297 10 min by switching off the 650 nm illumination and exciting with light from a slide projector
298 filtered through a 500 nm narrow band filter (Ealing Electro-Optics, Inc. Holliston, MA, USA)
299 and a 600 nm short-pass filter (Corion SL600, Newport Corp.). Fluorescence emission was
300 recorded with a QEPro spectrometer. The average rate of increase in SOSG fluorescence
301 between 535 and 540 nm during three consecutive 10 min red-light illumination periods was
302 taken as a relative rate of ¹O₂ production. Values were then averaged between three

303 independent biological replicates. Control measurements were done from illuminated samples
304 containing no algal cells and from algal cell samples incubated in the dark.

305

306 Photoinhibition of PSII

307

308 Light-induced loss of PSII activity was measured from algal samples diluted to OD₇₃₀ of 0.5.
309 A 10 ml sample was subjected to strong light (PPFD 950 $\mu\text{mol m}^{-2} \text{s}^{-1}$) from a 1000 W low-
310 pressure Xenon lamp (201-1k, 1000 W, Science tech inc, London, ON, Canada) equipped with
311 an ultraviolet protection film (Long Life for Art, Eichstetten, Germany) and a 9-cm water filter
312 to remove heat. The light path in the sample was 7 mm and the temperature was maintained at
313 25 °C throughout the experiment. The light-saturated rate of oxygen evolution (H_2O to DMBQ)
314 was measured from a 1 ml aliquot before illumination and during illumination every 10 min.
315 Lincomycin, when present, was used at 0.5 mg ml⁻¹ and added before the measurement of the
316 control rate of oxygen evolution. For comparison of the rates, the measured oxygen evolution
317 rates were first divided by the Chl concentration and then by the control value of the respective
318 sample. The loss of oxygen evolution in the presence of lincomycin was fitted to a first-order
319 reaction equation to obtain the rate constant of the damaging reaction of photoinhibition of
320 PSII (k_{PI}). The measurements were conducted with three independent biological replicates
321 from all conditions.

322

323 Results

324

325 Variation within the cultures contributes to survival and growth in extreme light

326

327 Transfer of *C. reinhardtii* cultures from PPFD 100 to 3000 $\mu\text{mol m}^{-2} \text{s}^{-1}$ led first to death of
328 some cells, as indicated by a decrease in OD_{730} during the first 24 h in EL (Fig. 1a). Thereafter,
329 however, most cultures resumed growth. Isolated subpopulations were more likely to acclimate
330 to extreme light within 96 hours than cultures originating from single cells (Table 1). After 96
331 hours in EL, the average OD_{730} of single-cell-originating cultures was 0.09 ± 0.02 (Fig. 1a),
332 whereas the average OD_{730} of isolated subpopulations was 0.18 ± 0.02 . These numbers only
333 include cultures that reached the OD_{730} level of 0.05 within 96 hours of transfer to EL, and only
334 such cultures were used in further experiments. However, we noted that practically all EL-
335 exposed cultures eventually started to grow if the exposure to EL continued. After 96 h, control
336 cultures that were kept in moderate light had reached the OD_{730} of 0.259 ± 0.003 , a significantly
337 higher cell density than either of the EL grown cultures ($P \ll 0.05$).

338 We also tested if the acclimation response was permanent by transferring 10 EL cultures to low
339 light for 7 days and then re-introducing them to the EL conditions. Not all cultures grew in the
340 same, EL-tolerating manner as previously (Fig. 1b). On average, the cultures that withstood the
341 re-introduction to extreme light had the OD_{730} of 0.172 ± 0.09 , similar as the density the
342 isolated subpopulations at the same time point after onset of the first EL treatment.

343

344 Acclimation lowers the amount of Chl but does not affect the amount of carotenoids

345

346 The sum of Chls *a* and *b* in cell cultures of the same OD_{730} decreased to one half during the
347 acclimation to EL (Fig. 2a), indicating a decrease in Chl per cell. The Chl *a/b* ratio did not

348 change in response to the acclimation (Fig. 2b). In some cultures, the amount of carotenoids
349 per cell remained rather constant during acclimation to EL, which led to doubling of the
350 carotenoid to Chl ratio (Fig. 2c). The pigment analysis showed no differences between EL-
351 exposed cultures originating from the two types of inocula (Fig. 2).

352 As all EL cultures, whether they originated from single cells or isolated subpopulations,
353 obviously shared the same phenotype, EL cultures for all further experiments were prepared
354 with the isolated subpopulation method.

355

356 Ratio of PSII to PSI fluorescence emission decreases during EL acclimation

357

358 Fluorescence emission was measured at the temperature of 77 K to see how the stoichiometry
359 of PSII and PSI behaves when the cells acclimate to EL. The results (Fig. 1c) show that the
360 ratio of fluorescence originating from PSII to fluorescence from PSI decreased from 1.5 in
361 control cells to 0.95 in EL cells as result of the acclimation.

362

363 PQ-to-Chl ratio is higher in EL than in control cells

364

365 PQ is an electron carrier molecule in the thylakoid membrane but in plants (Kruk and Karpinski
366 2006) and cyanobacteria (Khorobrykh et al. 2020), a large part of PQ is located outside of the
367 thylakoid membrane and does not take part in electron transfer. In plants, this non-photoactive
368 PQ is found in plastoglobuli and in the inner chloroplast envelope. We measured the amount
369 of PQ and found that the PQ-to-Chl ratio was approximately three-fold as high in EL as in
370 control cells (Fig. 1d). Comparison of Figs. 1d and 2a reveals that the amount of PQ per cell is

371 higher in EL than in control cells, as the ratio of the chlorophyll contents of control and EL
372 cells is approximately two.

373

374 Number of photosystems decreases in response to the EL acclimation

375

376 Decrease in total number of photosystems is a known response to increasing light intensity,
377 and PSI has been shown to be more heavily downregulated than PSII during high-light
378 cultivation of *C. reinhardtii* (Bonente et al. 2012). In the EL acclimation, the number of both
379 photosystems was found to decrease. Judging from the quantification of Western blots of the
380 CP43 and PsaA proteins, the PSII and PSI contents of the EL cells were 44.5 ± 16.7 % and
381 60.2 ± 14.6 % of the control cells, respectively (Fig. 3). These numbers match with the overall
382 reduction in the amount of chlorophyll to about one half during EL acclimation (Fig. 2a).

383

384 EL acclimated cells do not reduce artificial quinone electron acceptors efficiently

385

386 PSII can reduce a range of electron acceptors in addition to the natural acceptor PQ, and we
387 hypothesized that acclimation to EL might change the affinity of PSII to artificial electron
388 acceptors. To test this, the light-saturated rate of oxygen evolution was measured from control
389 and EL cells using different electron acceptors. To avoid changes in the cultures after the EL
390 treatment, the measurements were done immediately after removing an aliquot from the EL
391 culture and diluting to the standard OD₇₃₀ of 0.5. The time-consuming quantification of Chl
392 was done subsequently from parallel aliquots, and the average Chl concentrations of the control
393 and EL samples were 11.08 ± 0.40 and 3.89 ± 0.33 $\mu\text{g ml}^{-1}$, respectively.

394 Without artificial quinone electron acceptors, photosynthetic oxygen evolution, measured on
395 Chl basis, was twice as fast in EL as in control cultures (Fig. 4a). When measured on per OD₇₃₀
396 basis, approximating the relative rates per cell (the average cell density of the samples was 4.07
397 $\pm 0.059 \times 10^6$ cells ml⁻¹), the light-saturated rate of photosynthetic oxygen production turned
398 out to be faster in the control than in the EL cells instead (Fig. 4b). However, very low oxygen
399 evolution rates were measured from the EL cells when artificial PSII electron acceptor
400 quinones of any kind were used. The highest rate was obtained with DMBQ whereas rates
401 measured with the standard combination of DCBQ and FeCy, where the latter is included to
402 keep DCBQ oxidized, yielded a very low rate (Fig. 4). DCBQ-dependent oxygen evolution
403 continued both in control and EL cells upon addition of DBMIB, an inhibitor of oxidation of
404 PQH₂ at the cytochrome *b₆/f* complex; in fact, a higher rate was measured from control cells in
405 the presence of both DCBQ and DBMIB than with DCBQ alone. Photosynthetic oxygen
406 evolution, measured without artificial PSII electron acceptors, was effectively inhibited *in vivo*
407 by 0.5 μ M DBMIB in both types of cells.

408 To test if the tested artificial quinones simply cannot penetrate to EL cells, we also measured
409 oxygen evolution from isolated thylakoids. These measurements showed similar results as *in*
410 *vivo*, as thylakoids isolated from EL cells produced less oxygen than control cells with both
411 quinone electron acceptors (Fig. 4c), although the difference between control and EL
412 thylakoids was less drastic than that between control and EL cells (Fig. 4).

413

414 EL acclimation changes Chl *a* fluorescence kinetics

415

416 A single turnover flash causes electron transfer to the Q_A quinone of PSII, and the fluorescence
417 yield after the flash probes the oxidation of Q_A⁻. The first, most rapid phase of the decrease in

418 Chl *a* fluorescence yield after the single turnover flash was larger in EL samples than in the
419 control samples (Fig. 5a). When the samples were supplemented with DCMU, an inhibitor that
420 blocks electron transfer from Q_A to Q_B , EL cells showed slower decrease of fluorescence than
421 the control cells (Fig. 5b). The rate constant of recombination of the $S_2Q_A^-$ state, obtained by
422 fitting the curves measured in the presence of DCMU to a first-order equation, was 0.24 s^{-1} for
423 the control and only 0.08 s^{-1} for the EL cells.

424 Chl *a* fluorescence induction was very different in EL cells than in the control cells (Fig. 5c).
425 When fluorescence induction was measured in the absence of DCMU, EL cells had a much
426 higher F_0 level but a similar F_M level as control cells, and consequently the F_V/F_M value of the
427 EL cells (0.30 ± 0.04) was much lower than that of the control cells (0.76 ± 0.00) (Fig. 5c). In
428 the presence of DCMU, lower F_V/F_M values were obtained from both types of cells than in the
429 absence of DCMU, but the difference between EL and control cells remained similar as in the
430 absence of DCMU. A decrease in fluorescence yield after the maximum was observed in the
431 EL cells both in the absence and presence of DCMU (Figs. 5c and 5d).

432 Examination of the OJIP kinetics shows that in EL cells, the O-J-transition comprised most of
433 the initial fluorescence rise and no J-I-transition could be resolved (Fig. S2), whereas the
434 control cells expressed standard behavior of fluorescence induction. In the absence of DCMU,
435 both types of cells showed maximal fluorescence at the same time point of 161 ms. In the
436 presence of DCMU, fluorescence yield was higher in EL than in control cells (Fig. 5d).

437

438 Acclimation induces minor changes in thermoluminescence

439

440 The slow recombination of the $S_2Q_A^-$ state prompted us to use thermoluminescence to measure
441 eventual differences in the redox potentials of the PSII electron acceptors. The
442 thermoluminescence B band is associated with the $S_{2,3}Q_B^- \rightarrow S_{1,2}Q_B$ recombination and the Q
443 band with the $S_{2,3}Q_A^- \rightarrow S_{1,2}Q_A$ recombination. The Q band peaked at 13.6 °C in EL cells and
444 15.5 °C in control cells (Fig. 6), and the B band of the EL cells peaked at 21.6 °C, whereas the
445 B band of control peaked at 20.0 °C. Furthermore, the B band of the EL cells was wider than
446 that of the control cells. The quality of the thermoluminescence data did not allow fitting, but
447 a simulation of the behavior of a first-order thermoluminescence band showed that a lower pre-
448 exponential factor of Arrhenius's equation might explain why the B band of the EL cells was
449 wider and shifted to a higher temperature, compared to control cells (Fig. 6b and 6c).

450

451 EL acclimated cells produce less singlet oxygen than control cells

452

453 Reactive oxygen species are produced in chloroplasts in the light, and especially in strong light,
454 and 1O_2 production by PSII depends on recombination reactions that lead to the triplet state of
455 P_{680} (Krieger-Liszkay et al. 2008). The slow $S_2Q_A^-$ recombination in the EL cells (Fig. 5b)
456 might therefore predict a low 1O_2 yield. We used SOSG to measure 1O_2 production from control
457 and EL cells. For the measurement, a cell suspension was supplied with SOSG and illuminated
458 with high-intensity red light (PPFD 2000 $\mu\text{mol m}^{-2} \text{s}^{-1}$, >650 nm) that does not induce 1O_2
459 production by SOSG itself (Hakala-Yatkin and Tyystjärvi 2011). Both control and EL cells
460 produced 1O_2 at essentially constant rates throughout the 30-min illumination period. However,
461 the rate of 1O_2 production by an EL cell suspension was only 10.2 % of that of control cells,
462 when suspensions containing the same amount of Chl were compared (Fig. 7).

463

464 EL tolerance is not accompanied by a slow damaging reaction of photoinhibition

465

466 Effect of light on PSII activity was measured both in the presence and absence of lincomycin
467 that blocks the repair of PSII. Cells were illuminated at PPFD $950 \mu\text{mol m}^{-2} \text{s}^{-1}$ and PSII oxygen
468 evolution was measured from aliquots of the illuminated suspension with Chl concentrations
469 of $8.93 \pm 0.56 \mu\text{g ml}^{-1}$ and $4.87 \pm 0.78 \mu\text{g ml}^{-1}$ for control and EL samples, respectively. DMBQ
470 was used as electron acceptor. Again, DMBQ-dependent oxygen evolution, measured before
471 the illumination treatment, was much slower in EL than in control cells.

472 Illumination of cells in the presence of lincomycin led to a clear first-order decay of PSII
473 oxygen evolution activity in both types of cells (Fig. 8a). The rate of loss of PSII activity was
474 similar in both EL and control cells, with k_{PI} values of $1.47 \pm 0.12 \times 10^{-3} \text{s}^{-1}$ and $1.38 \pm 0.09 \times$
475 10^{-3}s^{-1} in control and EL samples, respectively (Fig. 8a, inset). Thus, the damaging reaction of
476 photoinhibition had the same rate in EL and control cells.

477 When the loss of active PSII units was measured under the same PPFD in the absence of
478 lincomycin, EL cells were, as expected, hardly affected (Fig. 8b, inset). Control cells, in turn,
479 rapidly lost PSII activity, and already after 20 min of illumination, both cell types had roughly
480 the same rate of oxygen production (Fig. 8b). Finally, the damaging reaction and repair of PSII
481 equilibrated in both control and EL samples to a similar oxygen production rate, 21.57 ± 4.5
482 and $22.29 \pm 5.6 \mu\text{mol (O}_2\text{)} \mu\text{g (Chl)}^{-1} \text{h}^{-1}$ for control and EL cells, respectively. The result may
483 suggest that the low $^1\text{O}_2$ production of the EL cells exerts its advantageous effect on translation
484 of chloroplast proteins (Nishiyama et al. 2001) only during a long cultivation in EL but not yet
485 during a short-time photoinhibition experiment.

486

487 Discussion

488

489 How does *C. reinhardtii* turn tolerant to an extreme light intensity

490

491 Effects of exposure of photosynthetic organisms to high light for a few hours has been studied
492 extensively (for review, see Tyystjärvi 2013), and also acclimation to strong but not extreme
493 light is a thoroughly studied topic in both plants and green algae (Bonente et al. 2012, Kouřil
494 et al. 2013, Dietz 2015, Belgio et al. 2018, Virtanen et al. 2019). However, less is known about
495 how organisms cope with prolonged exposure to light intensities highly exceeding full sunlight.
496 In fact, it was only recently shown that the optimum PPFD for biomass production by *C.*
497 *reinhardtii* is closer to 800 $\mu\text{mol m}^{-2} \text{s}^{-1}$ (Virtanen et al. 2019) than the moderate PPFD values
498 of 80-200 $\mu\text{mol m}^{-2} \text{s}^{-1}$ usually applied in cultivation of the alga. Here we examined how wild-
499 type *C. reinhardtii* reacts when suddenly transferred to PPFD 3000 $\mu\text{mol m}^{-2} \text{s}^{-1}$ after
500 precultivation at PPFD 100 $\mu\text{mol m}^{-2} \text{s}^{-1}$.

501 The first finding was that although *C. reinhardtii* stops growing when suddenly exposed to
502 extreme light intensity, growth resumes after a few days in the majority of culture bottles (Fig.
503 1a). The phenomenon was found to be so common, even when using cultures originating from
504 single cells as inocula (Table 1), that mutation can be excluded as a cause. The finding that the
505 rapidly obtained high-light tolerance is tuned down in a week, and in some cases even lost,
506 supports this conclusion (Table 1, Fig. 1b). However, this finding does not exclude the
507 possibility that acclimation to high light by mutations also occurs, as reported in earlier
508 publications (Förster et al. 2005, Schierenbeck et al. 2015).

509 The finding that isolated subpopulations acclimate more rapidly and, in terms of growth,
510 remain 24 hours ahead of the cultivations started from individual cells, suggests that
511 acclimation to extreme light has a genetic/epigenetic component. Actual genetic variation
512 within a *C. reinhardtii* culture is unlikely, as the maintenance cultivation does not induce sexual
513 reproduction, making epigenetic modification a more appealing explanation. Epigenetic
514 regulation is also in line with the slowly reversible nature of the observed, EL-acclimated state.
515 Epigenetic differences might be induced by subtle differences in the interplay between the
516 environment and developmental phase between individual cells during maintenance. It has
517 already been shown that the amount of epigenetic variation in a *C. reinhardtii* population can
518 contribute to its capability to acclimate to different environmental stress factors (Kronholm et
519 al. 2017; Duarte-Aké et al. 2018). In addition, the chloroplast genome of *C. reinhardtii* has
520 been reported to be especially prone to modification via methylation by DNA
521 methyltransferase DMT 1 (Nishiyama et al. 2002, 2004). It is also possible that the methylation
522 states of key genes change occur during the acclimation period, as the time window of
523 epigenetic regulation in *C. reinhardtii* (Umen and Goodenough 2001) matches with the time
524 that it takes for cultures to start growing in EL.

525

526 Physiological features of EL acclimated cells

527

528 The differences in the properties of *C. reinhardtii* cells before and after EL acclimation may
529 obviously reflect stress, acclimation, or both. The decrease in the Chl content of the cells might
530 indicate reduction in the antenna size that, in turn, would reduce the so-called excess excitation
531 energy absorbed by the photosynthetic machinery (Öquist et al. 1993). The change in the Chl
532 *a/b* ratio would indicate an alteration in the functional size of the antenna (Kirst et al. 2012).
533 However, this ratio remains constant throughout the acclimation (Fig. 2b), suggesting that the

534 EL-acclimated cells retain the functional size of their antennae. In agreement with the stable
535 Chl *a/b* ratio, the finding that the amounts of photosystems decrease during EL acclimation
536 approximately as much as the amount of chlorophyll (Figs. 3 and 2) suggest that the overall
537 number of photosystems per cell decreases during EL acclimation but the amount of Chl
538 associated with each photosystem remains stable.

539 In addition to the overall decrease of the photosystems, the 77 K fluorescence (Fig. 1c) and
540 Western blot data (Fig. 3) suggest that PSII units decrease more than PSI units. The most
541 straightforward interpretation for the low amount of PSII in the EL cells is that the EL treatment
542 causes so rapid photoinhibition that the repair of PSII fails to maintain full activity, and
543 eventually some PSII units become completely degraded. This interpretation is in agreement
544 with the finding that the rate of the damaging reaction of photoinhibition of PSII is the same in
545 EL and control cells (Fig. 8a, inset). Furthermore, the fluorescence induction data show that
546 most PSII centers of the EL cells are in an inactive, photoinhibited state, as the F_v/F_M ratio is
547 very low and the OJIP curves closely resemble curves obtained in the presence of DCMU (Fig.
548 5c and 5d). In addition, the finding that the amount of PQ per cell shows a slight increase during
549 EL acclimation (Fig. 1d) suggests that the number of PSII units decreases without a
550 simultaneous change in the amount of plastoquinone in the thylakoid membranes.

551 Intriguingly, these data are contrary to what happens in *C. reinhardtii* during a long-time
552 acclimation to high but not extreme light intensity (Bonente et al. 2012, Virtanen et al. 2019),
553 where the ratio of PSII to PSI increases, indicating a more drastic decrease in PSI than in PSII
554 units. However, here we observe also decrease in PSI content (Fig. 3). In addition, LHCSR3
555 accumulates in high light (Tibiletti et al. 2016), which is most probably the case also in EL
556 conditions, where it protects both photosystems by inducing NPQ (Girolomoni et al. 2019).
557 The combination of photoinhibition and NPQ probably cause PSII fluorescence to decrease
558 more than PSI fluorescence during EL treatment and acclimation.

559 Drastic decrease in the rate of production of $^1\text{O}_2$ in extreme light (Fig. 7) is most obviously a
560 high-light acclimation response. $^1\text{O}_2$ is mainly generated by PSII (Krieger-Lizkay 2005; Telfer
561 2014) and besides functioning as a general agent of harmful oxidation, $^1\text{O}_2$ is known to
562 specifically oxidize cyanobacterial translation elongation factors (Kojima et al. 2007), which
563 suggests that $^1\text{O}_2$ slows down PSII repair also in chloroplasts by interfering with chloroplast
564 protein synthesis (Nishiyama et al. 2001, Hakala-Yatkin et al. 2011). $^1\text{O}_2$ has also been
565 suggested to directly damage PSII in photoinhibition (Vass 2011). However, the low $^1\text{O}_2$ levels
566 in EL cells did not slow down the damaging reaction of photoinhibition in EL *C. reinhardtii*
567 (Fig. 8), suggesting that $^1\text{O}_2$ is not a crucial factor in determining the rate of photoinhibition.

568 Slow $^1\text{O}_2$ production is a common feature in both EL acclimated *C. reinhardtii* and *Chlorella*
569 *ohadii*, a green alga famous for being resistant both to strong light and photoinhibition of PSII
570 (Treves et al. 2016). However, the mechanisms of high-light tolerance in these two species of
571 algae are most probably different. In *C. ohadii*, the PSII antenna is small and the charge
572 recombination reactions are less likely to produce triplet states than in PSII found in other
573 autotrophs (Treves et al. 2016). The thermoluminescence data from EL cells of *C. reinhardtii*,
574 in contrast, indicate neither a decrease in the redox potential gap between $\text{Q}_\text{A}/\text{Q}_\text{A}^-$ and $\text{Q}_\text{B}/\text{Q}_\text{B}^-$
575 pairs nor a positive shift in the potential of the $\text{Q}_\text{A}/\text{Q}_\text{A}^-$ pair (Fig. 6; see Rappaport et al. 2002
576 for the general interpretations), suggesting that the probability of triplet formation by PSII
577 recombination reactions is not altered by EL acclimation. However, the charge recombination
578 reactions themselves are affected, as the $\text{S}_2\text{Q}_\text{A}^- \rightarrow \text{S}_1\text{Q}_\text{A}$ recombination appears to be slower in
579 EL than in control cells (Fig. 5b), which may at least partly explain the low $^1\text{O}_2$ production
580 rate. The slower rate of recombination may, at least partially, be caused by a change in the pre-
581 exponential factor of the Arrhenius equation of the rate constant of recombination (Fig. 6). A
582 small pre-exponential factor would simply slow down the rate of $\text{S}_2\text{Q}_\text{A}^- \rightarrow \text{S}_1\text{Q}_\text{A}$ recombination
583 in EL cells, in comparison to control cells. PSII units of both a wild-type organism (Treves et

584 al. 2016) and mutants (Fufezan et al. 2007) have been shown to be functional in spite of
585 structural differences that cause variations in the redox potentials of PSII electron acceptors.
586 Therefore, acclimation-dependent changes affecting the pre-exponential factor would not be
587 surprising. Another obvious feature, and possibly more prominent one, to explain the low levels
588 of $^1\text{O}_2$ in EL cells is their very high carotenoid-to-Chl ratio (Fig. 2c). Carotenoids are important
589 scavengers of $^1\text{O}_2$ (Ramel et al. 2012), and may quench $^1\text{O}_2$ before it can be detected by a
590 reaction with SOSG to a degree. The sum of these two factors could be the cause for the
591 observed results from SOSG-dependent detection of $^1\text{O}_2$.

592 Interestingly, acclimation to EL is associated with a decreased ability to reduce artificial
593 quinone electron acceptors (Fig. 4), suggesting that the side chain of PQ is important for
594 maintaining a sufficient rate of electron transfer to PQ in EL cells. The rates of electron transfer
595 to artificial quinone electron acceptors are slower than photosynthesis in EL cells, indicating
596 that the tested artificial quinones, in addition to acting as poor electron acceptors of PSII in the
597 EL acclimated cells, also inhibit electron transfer to the natural PQ. The behavior of the
598 artificial quinones can be flexible, as e.g. DBMIB is known to be able to bypass its own
599 blockage and act also as an electron acceptor *in vitro* (Schansker et al. 2005). *In vivo*, however,
600 DBMIB primarily caused cessation of electron transfer from PSII and only oxygen
601 consumption was observed in its presence. Furthermore, 2,5-dimethylbenzoquinone, a sister
602 compound of DMBQ used here (2,6-dimethylbenzoquinone), interacts less strongly with the
603 Q_B binding site of PSII than DCBQ (Graan and Ort 1986), which may explain why a higher
604 electron transfer rate was obtained with DMBQ than with DCBQ.

605 The oxygen evolution measurements from isolated thylakoids confirmed that the slow rates of
606 electron transfer to the quinone acceptors was not caused by slow diffusion of the quinones to
607 EL acclimated cells. Furthermore, as the chlorophyll concentrations of the samples in the *in*
608 *vitro* experiments were the same, the number of PSII units in control and EL acclimated

609 samples was the same. Thus, the rate of oxygen evolution per PSII unit was also much slower
610 in EL cells than in the control cells *in vitro*. Together all these data strongly suggest that PSII
611 has changed in the acclimation process. We hypothesize that EL acclimation causes subtle
612 structural or conformational changes in PSII, causing the observed changes in reduction of
613 artificial quinone electron acceptors. It is tempting to also hypothesize that the differences
614 observed in the function of the acceptor side might be related to the slow rate of charge
615 recombination in the PSII of the EL cells.

616 Comparison of EL and control cells during high-light illumination in the absence of lincomycin
617 shows that the level at which PSII activity equilibrates in high light is not higher in EL than in
618 control cells (Fig. 8b). This equilibrium is reached as a result of concurrent damaging and
619 recovery reactions (Samuelsson et al. 1985; Greer and Laing 1988; for a review, see Campbell
620 and Tyystjärvi 2012), and the similarity of the equilibrium levels in EL and control cells
621 indicates that the recovery reactions run at the same rate in both cell types, when measured on
622 chlorophyll basis. However, during EL exposure, proportionally low PSII activity may be high
623 enough to support cellular functions, as light intensity is not limiting.

624 The $Q_A^-Q_B \rightarrow Q_AQ_B^-$ electron transfer reaction seems to be faster in EL than in control cells
625 (Fig. 5a), and the light-saturated rate of photosynthesis, with PQ as the electron acceptor of
626 PSII, is faster in EL than in control cells if measured on per Chl basis (Fig. 4). However, on a
627 per cell basis, the rate of photosynthesis of EL cells appears to be slower than in control cells,
628 as the amount of Chl per cell decreases to one half during the EL acclimation (Fig. 2a).

629 The fluorescence induction curves (Fig. 5c) of EL cells reveal a rapid decrease in fluorescence
630 yield right after the peak fluorescence value. A similar although milder response is seen in the
631 presence of DCMU (Fig. 5d). Induction of LHCSR3-dependent non-photochemical quenching
632 may explain why fluorescence yield decreases in the absence of DCMU, as this type of NPQ

633 takes more than the applied 15 min dark-incubation to relax (Allorent et al. 2013). The decrease
634 in the presence of DCMU, in turn, might reflect light-induced enhancement of fluorescence
635 quenching by the inactive, severely photoinhibited PSII centers. The overall reduction of PSII
636 electron acceptors during OJIP measurements occurs at similar pace in both types of cells,
637 indicated by the similar time it took the fluorescence to reach the F_M level (Fig. 5c). These data
638 add further evidence for the suggestion that PSII is a target of the EL-acclimation process.

639

640 Conclusions

641

642 The results of the present study show that a culture of wild-type *C. reinhardtii* cells can rapidly
643 acclimate to extreme PPFD as high as 1.5 times direct sunlight, or 10-20 times the usual
644 cultivation PPFD. The acclimation mechanism shows signs suggesting involvement of
645 epigenetic variation present in the algal population. The EL acclimated phenotype has less both
646 photosystems per cell and a higher carotenoid-to-chlorophyll ratio than the control cells.
647 Furthermore, PSII charge recombination reactions in EL acclimated cells are slow, possibly
648 due to conformational changes that affect the pre-exponential Arrhenius factor of the rate
649 constant of charge recombination, rather than changes in redox potentials of the electron
650 carriers. Slow charge recombination and high carotenoid-to-Chl ratio probably explain why the
651 EL cells also show a low 1O_2 production rate. Low rate of 1O_2 production in high light is
652 expected to keep the recovery of photoinhibited PSII functional during growth in EL. On the
653 other hand, the rate of the damaging reaction of photoinhibition of PSII is similar in EL
654 acclimated and control cells.

655

656 References

- 657 Allen JF (1992) Protein phosphorylation in photosynthesis. *Biochim Biophys Acta* 1098:275-335.
658 [https://doi.org/10.1016/S0005-2728\(09\)91014-3](https://doi.org/10.1016/S0005-2728(09)91014-3)
- 659 Alloreant G, Ruytaro T, Roach T, et al (2013) A dual-strategy to cope with high light in
660 *Chlamydomonas reinhardtii*. *Plant Cell* 25:545-557. <https://doi.org/10.1105/tpc.112.108274>
- 661 Belgio E, Trsková E, Kotabová E, et al (2018) High light acclimation of *Chromera velia* points to
662 photoprotective NPQ. *Photosynth Res* 135:263-274. <https://doi.org/10.1007/s11120-017-0385-8>
- 663 Bonente G, Ballotari M, Truong TB, et al (2011) Analysis of LhcSR3, a protein essential for feedback
664 de-excitation in the green alga *Chlamydomonas reinhardtii*. *PLoS Biol* 9:e1000577.
665 <https://doi.org/10.1371/journal.pbio.1000577>
- 666 Bonente G, Pippa S, Castellano S, et al (2012) Acclimation of *C. reinhardtii* to different growth
667 irradiances. *J Biol Chem* 287:5833-5847. <https://doi.org/10.1074/jbc.M111.304279>
- 668 Cazzaniga S, Li Z, Niyogi KK, Bassi R, Dall'Osto L (2012) The Arabidopsis *szl1* mutant reveals a
669 critical role of β -carotene in Photosystem I photoprotection. *Plant Physiol* 159: 1745-1758
- 670 Campbell DA, Tyystjärvi E (2012) Parameterization of photosystem II photoinactivation and repair.
671 *Biochim Biophys Acta* 1817:258-265. <https://doi.org/10.1016/j.bbabi.2011.04.010>
- 672 Chukhutsina VU, Holtzwarth AR, Croce R (2019) Time-resolved fluorescence measurements on
673 leaves: principles and recent developments. *Photosynth Res* 140: 355-369.
674 <https://doi.org/10.1007/s11120-018-0607-8>
- 675 Delosme R, Olive J, Wollman FA (1996) Changes in light energy distribution upon state transitions:
676 an in vivo photoacoustic study of the wild type and photosynthesis mutants from *Chlamydomonas*
677 *reinhardtii*. *Biochim Biophys Acta* 1273:150-158. [https://doi.org/10.1016/0005-2728\(95\)00143-3](https://doi.org/10.1016/0005-2728(95)00143-3)

- 678 Dietz KJ (2015) Efficient high light acclimation involves rapid processes at multiple mechanistic
679 levels. *J Exp Bot* 66:2401-2414. <https://doi.org/10.1093/jxb/eru505>
- 680 Dimitrieva VA, Tyutereva EV, Voitsekhovkaja OV (2020) Singlet oxygen in plants: Generation,
681 detection and signaling roles. *Int J Mol Sci* 21:9. <https://doi.org/10.3390/ijms21093237>
- 682 Duarte-Aké F, Us-Casmas R, Cancino-García VJ, De-la-Peña C (2018) Epigenetic changes and
683 photosynthetic plasticity in response to environment. *Environ Exp Bot* 159:108-120.
684 <https://doi.org/10.1016/j.envexpbot.2018.12.010>
- 685 Förster B, Osmond CB, Pogson BJ (2005) Improved survival of very high light and oxidative stress is
686 conferred by spontaneous gain-of-function mutations in *Chlamydomonas*. *Biochim Biophys Acta*
687 1709:45-57. <https://doi.org/10.1016/j.bbabi.2005.05.012>
- 688 Fufezan C, Rutherford AW, Krieger-Liszkay A (2002) Singlet oxygen production in herbicide-treated
689 photosystem II. *FEBS Lett* 532:407-410. [https://doi.org/10.1016/S0014-5793\(02\)03724-9](https://doi.org/10.1016/S0014-5793(02)03724-9)
- 690 Fufezan C, Gross CM, Sjödin M, et al (2007) Influence of the redox potential of the primary quinone
691 acceptor on photoinhibition in photosystem II. *J Biol Chem* 282:12492-12502.
692 <https://doi.org/10.1074/jbc.M610951200>
- 693 Girolomoni L, Cazzaniga S, Pinnola A, et al (2019) LHCSR3 is a nonphotochemical quencher of both
694 photosystems in *Chlamydomonas reinhardtii*. *PNAS* 116:4212-4217.
695 <https://doi.org/10.1073/pnas.1809812116>
- 696 Gorman DS, Levine RP (1965) Cytochrome f and plastocyanin: their sequence in the photosynthetic
697 electron transport chain of *Chlamydomonas reinhardtii*. *Proc Natl Acad Sci* 54:1665-1669.
698 <https://doi.org/10.1073/pnas.54.6.1665>
- 699 Graan T, Ort DR (1986) Detection of oxygen-evolving photosystem II centers inactive in
700 plastoquinone reduction. *Biochim Biophys Acta* 852:320-330. [https://doi.org/10.1016/0005-](https://doi.org/10.1016/0005-2728(86)90238-0)
701 [2728\(86\)90238-0](https://doi.org/10.1016/0005-2728(86)90238-0)

- 702 Greer DH, Laing WA (1988) Photoinhibition of photosynthesis in intact kiwifruit (*Actinidia delicosa*)
703 leaves: changes in susceptibility to photoinhibition and recovery during the growth season. *Planta*
704 186:418-425. <https://doi.org/10.1007/BF00195323>
- 705 Hakala-Yatkin M, Sarvikas P, Paturi P, et al (2011) Magnetic field protects plants against high light
706 by slowing down production of singlet oxygen. *Physiol Plant* 142:26-34.
707 <https://doi.org/10.1111/j.1399-3054.2011.01453.x>
- 708 Hakala-Yatkin M, Tyystjärvi E (2011) Inhibition of Photosystem II by the singlet oxygen sensor
709 compounds TEMP and TEMPD. *Biochim Biophys Acta* 1807: 243-250
710 <https://doi.org/10.1016/j.bbabi.2010.11.014>
- 711 Havurinne V, Mattila H, Antinluoma M, Tyystjärvi E (2019) Unresolved quenching mechanism of
712 chlorophyll fluorescence may invalidate multiple turnover saturating pulse analyses of photosynthetic
713 electron transfer in microalgae. *Physiol Plant* 166: 365-379. <https://doi.org/10.1111/ppl.12829>
- 714 Hideg É, Vass I (1995) Singlet oxygen is not produced in photosystem I under photoinhibitory
715 conditions. *Photochem Photobiol* 62: 949-952. <https://doi.org/10.1111/j.1751-1097.1995.tb09162.x>
- 716 Hoops S, Sahle S, Gauges R et al (2006) COPASI: a COMplex PATHway SIMulator. *Bioinformatics*
717 22: 3067-3074. <https://doi.org/10.1093/bioinformatics/btl485>
- 718 Ivanov AG, Morgan RM, Gray GR, et al. (1998) Temperature/light dependent development of
719 selective resistance to photoinhibition of photosystem I. *FEBS Lett* 430:288-292.
720 [https://doi.org/10.1016/S0014-5793\(98\)00681-4](https://doi.org/10.1016/S0014-5793(98)00681-4)
- 721 Khorobrykh S, Tsurumaki T, Tanaka K, et al (2020) Measurement of the redox state of the
722 plastoquinone pool in cyanobacteria. *FEBS Lett* 594:367-375. [https://doi.org/10.1002/1873-](https://doi.org/10.1002/1873-3468.13605)
723 3468.13605

- 724 Kirst H, Garcia-Sedan JG, Zurbriggen A, et al (2012) Truncated photosystem chlorophyll antenna size
725 in the green microalga *Chlamydomonas reinhardtii* upon deletion of the *TLA3-CpSRP43* gene. *Plant*
726 *Physiol.* 160:2251-2260. <https://doi.org/10.1104/pp.112.206672>.
- 727 Kondo T, Pinnola A, Chen WJ, et al (2017) Single-molecule spectroscopy of LHCSR1 protein
728 dynamics identifies two distinct states responsible for multi-timescale photosynthetic photoprotection.
729 *Nat Chem* 9:772-778. <https://doi.org/10.1038/NCHEM.2818>
- 730 Kojima K, Oshita M, Nanjo Y, et al (2007) Oxidation of elongation factor G inhibits the synthesis of
731 the D1 protein of photosystem II. *Mol Microbiol* 65:936–947 <https://doi.wiley.com/10.1111/j.1365->
732 [2958.2007.05836.x](https://doi.wiley.com/10.1111/j.1365-2958.2007.05836.x)
- 733 Kouřil R, Wientjes E, Bultema JB, et al (2013) High-light vs. low-light: Effect of acclimation on
734 photosystem II composition and organization in *Arabidopsis thaliana*. *Biochim Biophys Acta*
735 1827:411-419. <https://dx.doi.org/10.1016/j.bbabi.2012.12.003>
- 736 Krieger-Lizkay A (2005) Singlet oxygen production in photosynthesis. *J Exp Bot* 56:337-346.
737 <https://doi.org/10.1093/jxb/erh237>
- 738 Krieger-Liszky A, Fufezan C, Trebst A (2008) Singlet oxygen production in photosystem II and
739 related protection mechanism. *Photosyn Res* 98:551-564. <https://doi.org/10.1007/s11120-008-9349-3>
- 740 Kronholm I, Bassett A, Baulcombe D, Collins S (2017) Epigenetic and genetic contributions to
741 adaptation in *Chlamydomonas*. *Mol Biol Evol* 34:2285-2306. <https://doi.org/10.1093/molbev/msx166>
- 742 Kruk J, Karpinski S (2006) An HPLC-based method of estimation of the total redox state of
743 plastoquinone in chloroplasts, the size of the photochemically active plastoquinone-pool and its redox
744 state in thylakoids of *Arabidopsis*. *Biochim Biophys Acta* 1757:1669-1675.
745 <https://doi.org/10.1016/j.bbabi.2006.08.004>

- 746 Liguori N, Roy LM, Opacic M et al (2013) Regulation of light-harvesting in the green alga
747 *Chlamydomonas reinhardtii*: The C-terminus of LHCSR is the knob of a dimmer switch. J Am Chem
748 Soc 135:18339-18342. <https://doi.org/10.1021/ja4107463>
- 749 Lima-Melo Y, Alencar CTCB, Lobo AKM, et al. (2019) Photoinhibition of Photosystem I provides
750 oxidative protection during imbalanced photosynthetic electron transport in *Arabidopsis thaliana*.
751 Front Plant Sci 10:916. <https://doi.org/10.3389/fpls.2019.00916>
- 752 Nagy G, Ünneper R, Zsiros O, et al (2014) Chloroplast remodeling during state transitions in
753 *Chlamydomonas reinhardtii* as revealed by noninvasive techniques in vivo. Proc Natl Acad Sci
754 111:5042-5047. <https://doi.org/10.1073/pnas.1322494111>
- 755 Nawrocki WJ, Liu X, Croce R (2019) *Chlamydomonas reinhardtii* exhibits de facto constitutive NPQ
756 capacity in physiologically relevant conditions. Plant Physiol 182:472-479.
757 <https://doi.org/10.1104/pp.19.00658>
- 758 Nishiyama R, Ito M, Yamaguchi Y, et al (2002) A chloroplast-resident DNA methyltransferase is
759 responsible for hypermethylation of chloroplast genes in *Chlamydomonas* maternal genes. Proc Natl
760 Acad Sci 99:5925-5930. <https://doi.org/10.1073/pnas.082120199>
- 761 Nishiyama R, Wada Y, Mibu M, et al (2004) Role of a nonselective *de novo* DNA methyltransferase
762 in maternal inheritance of chloroplast genes in the green alga, *Chlamydomonas reinhardtii*. Genetics
763 168:809-816. <https://doi.org/10.1534/genetics.104.030775>
- 764 Nishiyama Y, Yamamoto H, Allakhverdiev SI, et al (2001) Oxidative stress inhibits the repair of
765 photodamage to the photosynthetic machinery. EMBO J 20:5587-5594.
766 <https://doi.org/10.1093/emboj/20.20.5587>
- 767 Nishiyama Y, Allakhverdiev SI, Yamamamoto H, et al (2004) Singlet oxygen inhibits the repair of
768 photosystem II by suppressing the translation elongation of the D1 protein in *Synechocystis* sp.
769 PCC6803. Biochemistry 43:11321–11330. <https://doi.org/10.1021/bi036178q>

- 770 Peers G, Truong TB, Ostendorf E, et al (2009) An ancient light-harvesting protein is critical for the
771 regulation of algal photosynthesis. *Nature* 462:518-521. <https://doi.org/10.1038/nature08587>
- 772 Porra RJ, Thompson WA, Kriedemann PE (1989) Determination of accurate coefficients and
773 simultaneous equations for assaying chlorophylls *a* and *b* extracted with four different solvents:
774 verification of the concentration of chlorophyll standards by atomic spectroscopy. *Biochim Biophys*
775 *Acta* 975:384-394. [https://doi.org/10.1016/S0005-2728\(89\)80347-0](https://doi.org/10.1016/S0005-2728(89)80347-0).
- 776 Ramel F, Birtic S, Cuiné S, et al (2012) Chemical quenching of singlet oxygen by carotenoids. *Plant*
777 *Physiol* 158:1267-1278. <https://doi.org/10.1104/pp.111.182394>
- 778 Rappaport F, Guergova-Kuras M, Nixon PJ, et al. (2002) Kinetics and pathways of charge
779 recombination in Photosystem II. *Biochemistry* 41:8518-8527. <https://doi.org/10.1021/bi025725p>
- 780 Roach T, Na CS (2017) LHCSR3 affects de-coupling and re-coupling of LHCII to PSII during state
781 transitions in *Chlamydomonas reinhardtii*. *Sci Rep* 7:43145. <https://doi.org/10.1038/srep43145>
- 782 Samuelsson G, Lönneborg A, Rosenqvist E, et al (1985) Photoinhibition and reactivation of
783 photosynthesis in the cyanobacterium *Anacystis nidulans*. *Plant Physiol* 4:992-995.
784 <https://doi.org/10.1104/pp.79.4.992>
- 785 Sarvikas P, Hakala M, Pätsikkä E, et al (2006) Action spectrum of photoinhibition in leaves of wild-
786 type and *npq1-2* and *npq4-1* mutants of *Arabidopsis thaliana*. *Plant Cell Physiol* 47:391-400.
787 <https://doi.org/10.1093/pcp/pcj006>
- 788 Schansker G, Tóth SZ, Strasser RJ (2005) Methylviologen and dibromothymoquinone treatments of
789 pea leaves reveal the role of photosystem I in the Chl *a* fluorescence OJIP. *Biochim Biophys Acta*
790 1706:250-261. <https://doi.org/10.1016/j.bbabi.2004.11.006>
- 791 Schierenbeck L, Ries D, Rogge K, et al (2015) Fast forward genetics to identify mutations causing a
792 high light tolerant phenotype in *Chlamydomonas reinhardtii* by whole-genome-sequencing. *BMC*
793 *Genomics* 16:57. <https://doi.org/10.1186/s12864-015-1232-y>

- 794 Sejima T, Tagaki D, Fukayama H, Makino A, Miyake C (2014) Repetitive short-pulse light mainly
795 inactivates Photosystem I in sunflower leaves. *Plant Cell Physiol* 55: 1184-1193.
796 doi:10.1093/pcp/pcu061
- 797 Shimakawa G, Miyake C (2018) Oxidation of P700 ensures robust photosynthesis. *Front Plant Sci* 9:
798 1617. <https://doi.org/10.3389/fpls.2018.01617>
- 799 Sonoike K (2011) Photoinhibition of photosystem I. *Physiol Plant* 142:56-64.
800 <https://doi.org/10.1111/j.1399-3054.2010.01437.x>
- 801 Sueoka N (1960) Mitotic replication of deoxyribonucleic acid in *Chlamydomonas reinhardi*. *Proc*
802 *Natl Acad Sci* 46:83-91. <https://doi.org/10.1073/pnas.46.1.83>
- 803 Telfer A (2014) Singlet oxygen production by PSII under light stress: mechanism, detection and
804 protective role of β -carotene. *Plant Cell Physiol* 55:1216-1223. <https://doi.org/10.1093/pcp/pcu040>
- 805 Tian L, Nawrocki WJ, Liu X, et al (2019) pH dependence, kinetics and light-harvesting regulation of
806 nonphotochemical quenching in *Chlamydomonas*. *Proc Natl Acad Sci* 116:8320-8325.
807 <https://doi.org/10.1073/pnas.1817796116>
- 808 Tibiletti T, Auroy P, Peltier G et al (2016) *Chlamydomonas reinhardtii* PsbS protein is functional and
809 accumulates rapidly and transiently under high light. *Plant Physiol* 171:2717-2730.
810 <https://doi.org/10.1104/pp.16.00572>
- 811 Tilbrook K, Dubois M, Crocco CD, et al (2016) UV-B perception and acclimation in *Chlamydomonas*
812 *reinhardtii*. *Plant Cell* 4:966-983. <https://doi.org/10.1105/tpc.15.00287>
- 813 Tikkanen M, Aro EM (2014) Integrative regulatory network of plant thylakoid energy transduction.
814 *Trends in Plant Sci* 19:10-17. <https://doi.org/10.1016/j.tplants.2013.09.003>

- 815 Treves H, Raanan H, Kedem I, et al (2016) The mechanisms whereby the green alga *Chlorella ohadii*,
816 isolated from desert soil crust, exhibits unparalleled photodamage resistance. *New Phytol* 210:1229-
817 1243. <https://doi.org/10.1111/nph.13870>
- 818 Tyystjärvi E, Aro EM (1996) The rate constant of photoinhibition, measured in lincomycin-treated
819 leaves, is directly proportional to light intensity. *Proc Natl Acad Sci* 93:2213-2218.
820 <https://doi.org/10.1073/pnas.93.5.2213>
- 821 Tyystjärvi E, Rantamäki S, Tyystjärvi J (2009) Connectivity of photosystem II is the physical basis of
822 retrapping in photosynthetic thermoluminescence. *Biophys J* 96:3735-3743.
823 <https://doi.org/10.1016/j.bpj.2009.02.014>
- 824 Tyystjärvi E (2013) Photoinhibition of photosystem II. In: Jeon K (ed), *International Review Of Cell*
825 *and Molecular Biology*, Academic Press, Elsevier Inc., pp 243–303.
- 826 Umen J, Goodenough U (2001) Chloroplast DNA methylation and inheritance in *Chlamydomonas*.
827 *Genes Dev* 15:2585-2597. <https://doi.org/10.1101/gad.906701>
- 828 Vass I (2011) Role of charge recombination processes in photodamage and photoprotection of the
829 photosystem II complex. *Physiol Plant* 142:1-16. [https://doi.wiley.com/10.1111/j.1399-](https://doi.wiley.com/10.1111/j.1399-3054.2011.01454.x)
830 [3054.2011.01454.x](https://doi.wiley.com/10.1111/j.1399-3054.2011.01454.x)
- 831 Virtanen O, Valev D, Kruse O, et al (2019) Photoinhibition and continuous growth of the wild-type
832 and a high-light tolerant strain of *Chlamydomonas reinhardtii*. *Photosynthetica* 57:617-626.
833 <https://doi.org/10.32615/ps.2019.056>
- 834 Wellburn AR (1994) The spectral determination of chlorophylls *a* and *b*, as well as carotenoids, using
835 various solvents with spectrophotometers of different resolution. *J Plant Physiol* 144:307-313.
836 [https://doi.org/10.1016/S0176-1617\(11\)81192-2](https://doi.org/10.1016/S0176-1617(11)81192-2)
- 837 Wobbe L, Bass R, Kruse O (2016) Multi-level light capture control in plants and green algae. *Trends*
838 *Plant Sci* 21:55-68. <https://doi.org/10.1016/j.tplants.2015.10.004>

- 839 Öquist G, Hurry V, Huner NPA (1993) The temperature-dependence of the redox state of Q(A) and
840 susceptibility of photosynthesis to photoinhibition. *Plant Physiol Biochem* 31:683–691.
- 841 Sonoike K (2011) Photoinhibition of photosystem I. *Physiol Plant* 142:56-64. doi:10.1111/j.1399-
842 3054.2010.01437.x
- 843 Tyystjärvi E, Ovaska J, Karunen P, Aro E-M (1989) The nature of light-induced inhibition of
844 Photosystem II in pumpkin (*Cucurbita pepo* L.) depends on temperature. *Plant Physiol* 91:1069-1074.
- 845 Ünlü C, Drop B, Croce R, van Amerongen H (2014) State transitions in *Chlamydomonas reinhardtii*
846 strongly modulate the functional size of photosystem II but not of photosystem I. *Proc Natl Acad Sci*
847 111:3460-3465. <https://doi.org/10.1073/pnas.1319164111>

848 Figure legends

849

850 **Fig. 1 (a)** Growth of cultures of *C. reinhardtii* strain *cc124* in control conditions (open circles,
851 solid line) and two types of cultures in EL: isolated subpopulations (red circles, red dashed
852 line) and single-cell-originating inocula (red triangles, red dotted line). **(b)** the growth of
853 individual, EL-categorized, single-cell-originating cultures, after being cultured in moderate
854 PPFD of $100 \mu\text{mol m}^{-2} \text{s}^{-1}$ for 1 week after initial EL acclimation. The growth of the cultures
855 was determined spectrophotometrically as increase in optical density at 730 nm. The inoculum
856 density was 0.01, after which the cultures were kept for 96 hours in the light conditions
857 described. The cells were grown in 45 ml of photoautotrophic medium at room temperature
858 and ambient atmosphere on a shaker. The curves in **a** are averaged from 3 (control) or 30 (EL
859 cultures) independent biological replicates and the error bars show SEM. The curves in **b**
860 represent observations from individual cultures. **(c)** Fluorescence emission spectrum of control
861 (solid, black line) and EL cells (dashed, red line) measured at 77 K. The samples taken directly
862 from growth conditions were stored at $-80 \text{ }^\circ\text{C}$ and diluted to $1.5 \mu\text{g Chl ml}^{-1}$ and final volume
863 $50 \mu\text{l}$ upon measurement. Fluorescence was measured with QEPro spectrometer with 442 nm
864 excitation. The data were normalized to the value at 713 nm. **(d)** Total amount of PQ in control
865 (white bar) and EL (black bar) cells, normalized to Chl concentration. The total amount of PQ
866 was measured with a HPLC method (Khorobrykh et al. 2020) from cultures that had reached
867 the end of exponential growth phase; the Chl concentrations for the normalization were
868 measured spectrophotometrically from methanol extracts of the cultures. All the data in **c** and
869 **d** are averaged from three independent biological replicates and the error bars show SD.

870

871 **Fig. 2 (a)** Total concentration of Chls *a* and *b*, **(b)** ratio of Chls *a* and *b* and **(c)** ratio of total
872 carotenoids to Chls, measured from pre-condition grown control (white bars), and EL grown
873 isolated subpopulation (black bars) and single-cell-originating cultures (grey bars) of *C.*
874 *reinhardtii*. The pigments were extracted in cold (+4 °C) and darkness via methanol extraction
875 from cultures with OD₇₃₀ of 0.5. The samples were taken directly from the cultures grown in
876 control or EL conditions. The bars are averaged from three (control) or 15–17 (EL cultures)
877 biological replicates and the error bars show SD.

878

879 **Fig. 3** Detection of CP43 and PsaA proteins on a film **(a)** and quantification of these proteins
880 **(b)** from control (white bars) and EL (black bars) cells. Western blotting was done from
881 extracted total soluble proteins, and 1 µg (CP43) or 2 µg (PsaA) of total proteins were loaded
882 to SDS-PAGE per well. Binding of the primary and secondary antibodies was visualized via
883 luminescence emitted by alkaline phosphatase. The signals were normalized to the average of
884 signals originating from control samples of the respective western blot. Each bar represents an
885 average of three biological replicates and the error bars show SD.

886

887 **Fig. 4** PSII activity, measured as light-saturated oxygen evolution from control (white bars)
888 and EL samples of *C. reinhardtii* (black bars) both *in vivo* **(a, b)** and in isolated thylakoids **(c)**
889 with different electron acceptors and one inhibitor of electron transfer, normalized to Chl **(a,**
890 **c)** or cell **(b)** concentrations. Light-saturated oxygen evolution was measured at PPFD 2000
891 µmol m⁻² s⁻¹ from cultures with OD₇₃₀ of 0.5. The cultures were grown in PPFD of either 100
892 or 3000 µmol m⁻² s⁻¹ and 1 ml samples were used in measurement. Isolated thylakoids were
893 used in final chlorophyll concentration of 5 µg ml⁻¹. The concentrations of artificial electron
894 acceptors (DCBQ, FeCy and DMBQ) were 0.5 mM and the inhibitor (DBMIB) was added at

895 the concentration of 0.5 μM . Each bar represents an average of three biological replicates and
896 the error bars show SD (* = $P < 0.05$, *** = $P < 0.005$)

897

898 **Fig. 5** Decay of Chl *a* fluorescence yield after a single turnover flash (**a, b**) and fluorescence
899 signal of Chl *a* fluorescence induction (**c, d**) measured in the absence (**a, c**) and presence (**b, d**)
900 of DCMU from control (black, solid lines) and EL (red, dashed lines) *C. reinhardtii* cells in
901 ambient air. Fluorescence measurements were conducted with 2 ml samples of cells containing
902 either 5 $\mu\text{g Chl ml}^{-1}$ (fluorescence decay, panels **a, b**) or 1 $\mu\text{g Chl ml}^{-1}$ (fluorescence induction,
903 panels **c, d**). The samples were dark-incubated for 15 minutes before measurement. The values
904 in **a** and **b** are double normalized, first to the zero fluorescence level, measured before the flash,
905 and then to the maximum fluorescence after the single turnover flash given at $t = 1$ ms.
906 Fluorescence induction (**c, d**) was induced with blue, 455 nm actinic light with PPFD 400 μmol
907 $\text{m}^{-2} \text{s}^{-1}$. All curves are averaged from three independent biological replicates and the error bars
908 show SD.

909

910 **Fig. 6 (a)** Thermoluminescence Q band (solid line) and B band (dashed line) measured from
911 control (black) and EL (red) cultures of *C. reinhardtii*. 200 μl samples, containing 3.1 μg of
912 Chl, were cooled down to either -20 $^{\circ}\text{C}$ (for Q band measurements) or -10 $^{\circ}\text{C}$ (B band
913 measurements) and then charged with a single turnover flash. The temperature was then
914 gradually increased up to 60 $^{\circ}\text{C}$ at a heating rate of 0.66 $^{\circ}\text{C s}^{-1}$. The Q bands were recorded in
915 the presence of 20 μM DCMU. All bands are averaged from three biological replicates. (**b**)
916 Simulated thermoluminescence curves assuming a first-order reaction with $E_a = 501$ eV, heating
917 rate 0.66 $^{\circ}\text{C s}^{-1}$ and pre-exponential factor of Arrhenius' equation of $1.7 \times 10^7 \text{ s}^{-1}$ (solid line),

918 $1.2 \times 10^7 \text{ s}^{-1}$ (dashed line) or $9 \times 10^6 \text{ s}^{-1}$ (dotted line) and (c) the half width at half maximum of
919 the thermoluminescence band as a function of the pre-exponential factor.

920

921 **Fig. 7** $^1\text{O}_2$ production, measured as increase of fluorescence emitted by endoperoxidized
922 SOSG, of control (open circles) and EL cells (black circles) in comparison to light controls
923 illuminated without SOSG (grey bars) and dark controls (black bars) incubated in the dark with
924 SOSG. 350 μl samples containing $50 \mu\text{g ml}^{-1}$ Chl were supplemented with $50 \mu\text{M}$ SOSG and
925 then treated with red light ($> 650 \text{ nm}$) with PPFD $2000 \mu\text{mol m}^{-2} \text{ s}^{-1}$. The fluorescence emitted
926 by SOSG that had reacted with $^1\text{O}_2$ was excited with 500 nm light and recorded
927 spectrophotometrically at $535\text{-}540 \text{ nm}$. Each data point represents an average of three
928 biological replicates and the error bars show SD.

929

930 **Fig. 8** Photoinhibition of PSII *in vivo* measured as decrease in light-saturated oxygen evolution
931 in control (white bars) and EL (black bars) cultures of *C. reinhardtii*, illuminated in the
932 presence (a) and in the absence (b) of lincomycin. The insets show data from a and b when
933 normalized to the control value at $t=0$. Live cells, grown in either pre-culture or EL conditions,
934 as indicated, were collected and used at OD_{730} of 0.5 (cell density $4 \times 10^6 \text{ cells ml}^{-1}$, $8.9 \mu\text{g ml}^{-1}$
935 1 and $4.9 \mu\text{g ml}^{-1}$ Chl in control and EL samples, respectively). A 10 ml sample was treated
936 with photoinhibitory white light (PPFD $950 \mu\text{mol m}^{-2} \text{ s}^{-1}$) and a 1 ml aliquot was used to
937 quantify the number of active PSII units in the illuminated sample by measuring the rate of
938 light-saturated oxygen evolution (H_2O to DMBQ). 1 ml aliquots were supplemented with
939 DMBQ and FeCy in final concentration of 0.5 mM prior to measuring the oxygen evolution
940 rate. The lines in inset of a represent the best fit to the reaction equation describing the kinetics

941 of damaging reaction of photoinhibition. Each bar represents an average of three biological
942 replicates and the error bars show SD.

943

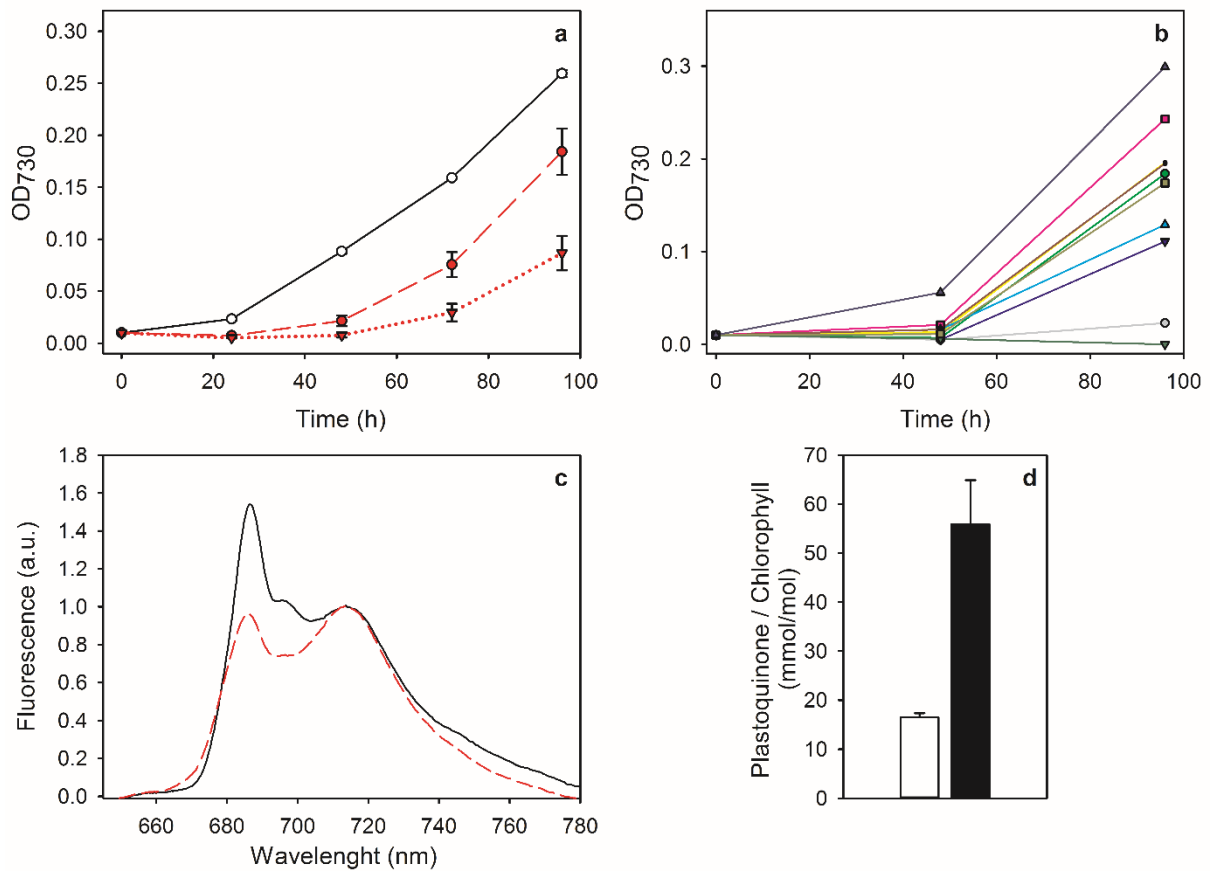
944 **Table 1 Statistics of *C. reinhardtii* cultures grown in EL (PPFD 3000 $\mu\text{mol m}^{-2} \text{s}^{-1}$).** The EL
 945 cultures were started as isolated subpopulation of the maintenance culture or from inocula
 946 grown separately starting from single cells, as indicated. Before shifting to EL, all cultures
 947 were diluted to OD₇₃₀ of 0.01.

948

	% of cultures that reached OD ₇₃₀ of 0.05 in 24 hours	% of cultures that reached OD ₇₃₀ of 0.05 in 48 hours	% of cultures that grew over OD ₇₃₀ of 0.05 in 96 hours
Cultures originating from single cells	0 %	3.3 %	56.7 %
Isolated subpopulations	0 %	13.3 %	80 %
HL-categorized cultures reintroduced to extreme light after 1 week in moderate light	-	10 %	80 %

949

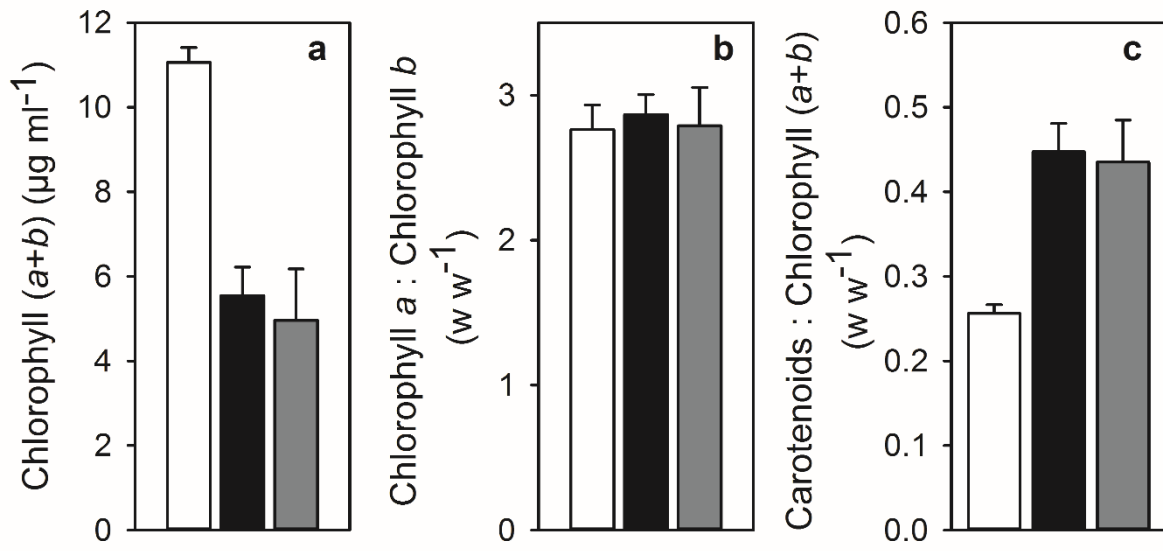
950



951

952 **Fig. 1**

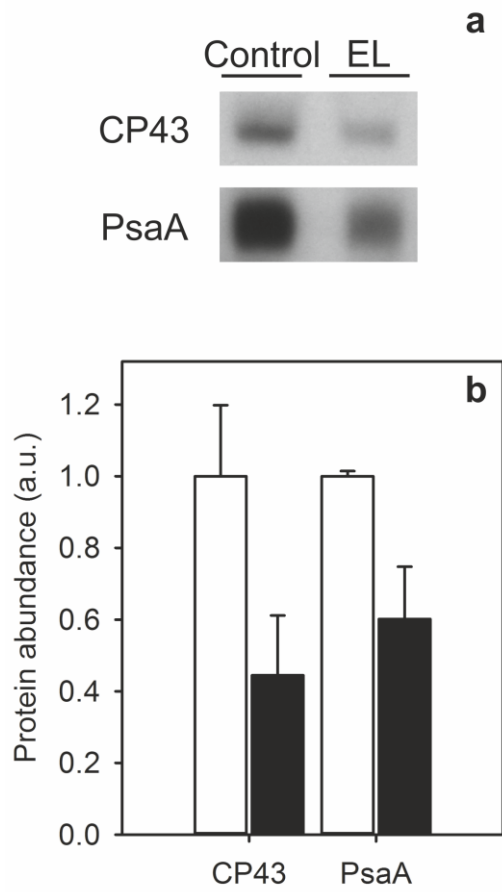
953



954

955 **Fig. 2.**

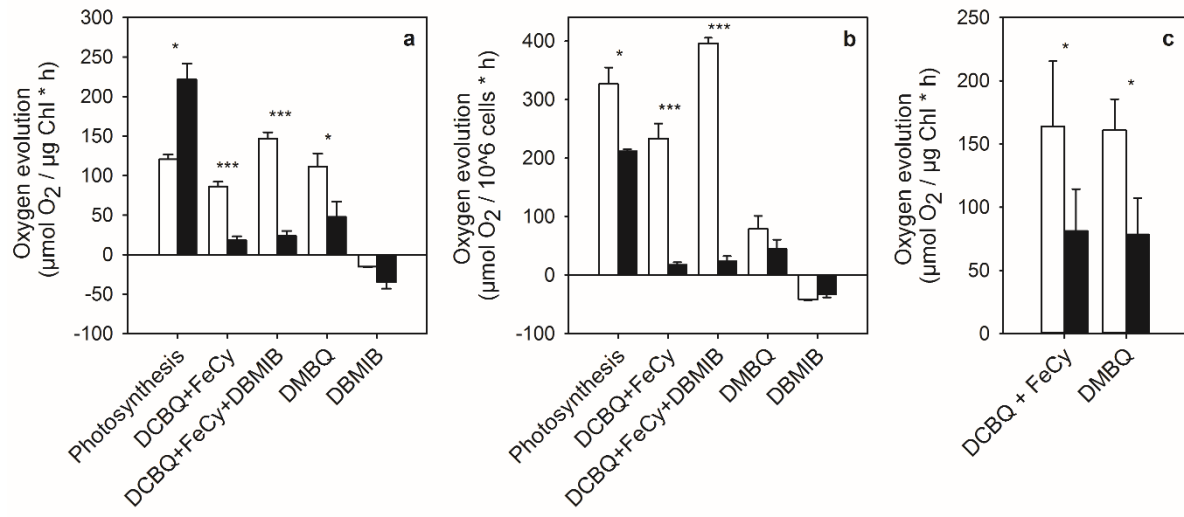
956



957

958 Fig. 3.

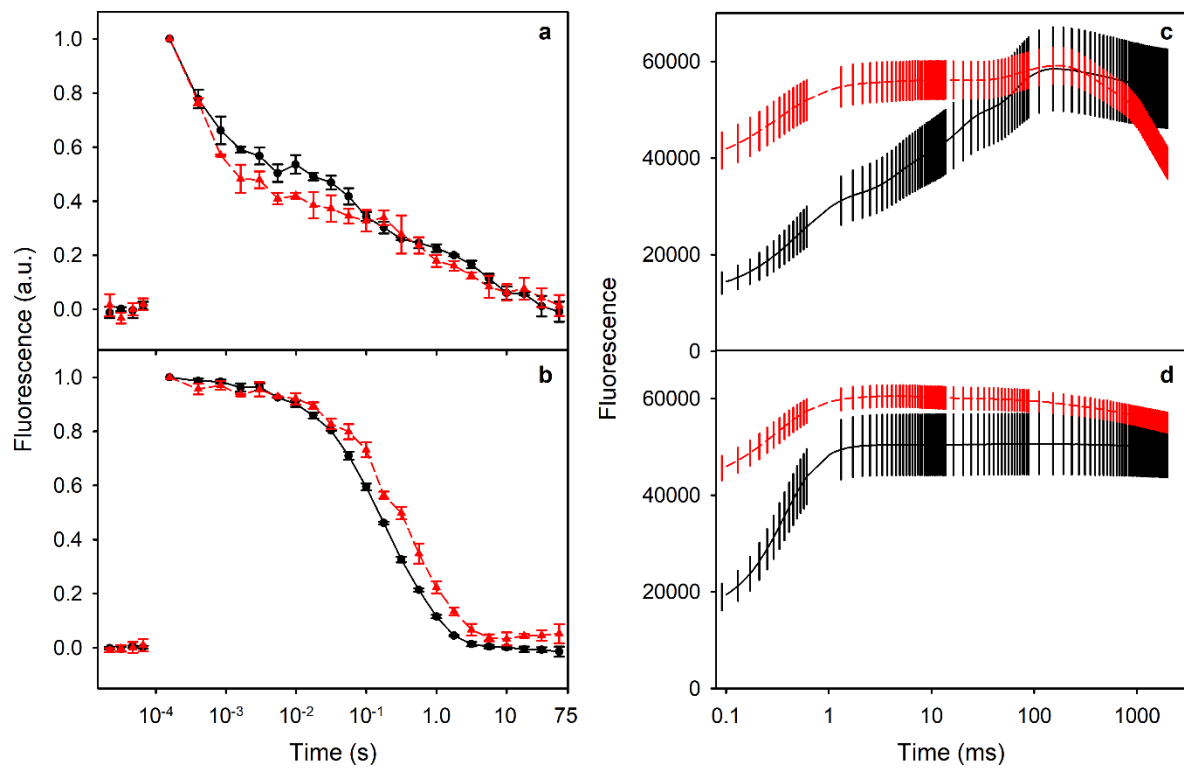
959



960

961 **Fig. 4.**

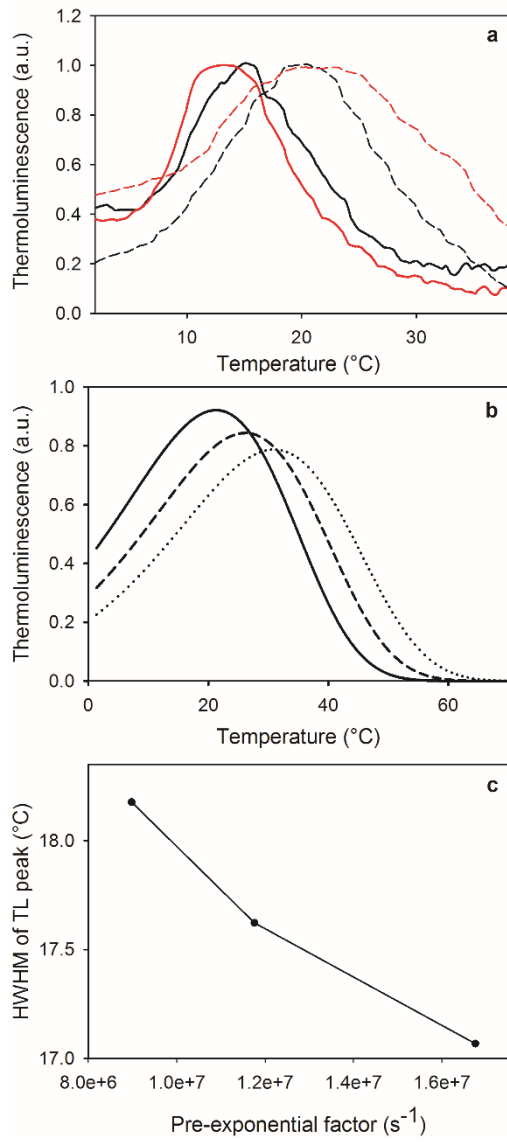
962



963

964 **Fig. 5.**

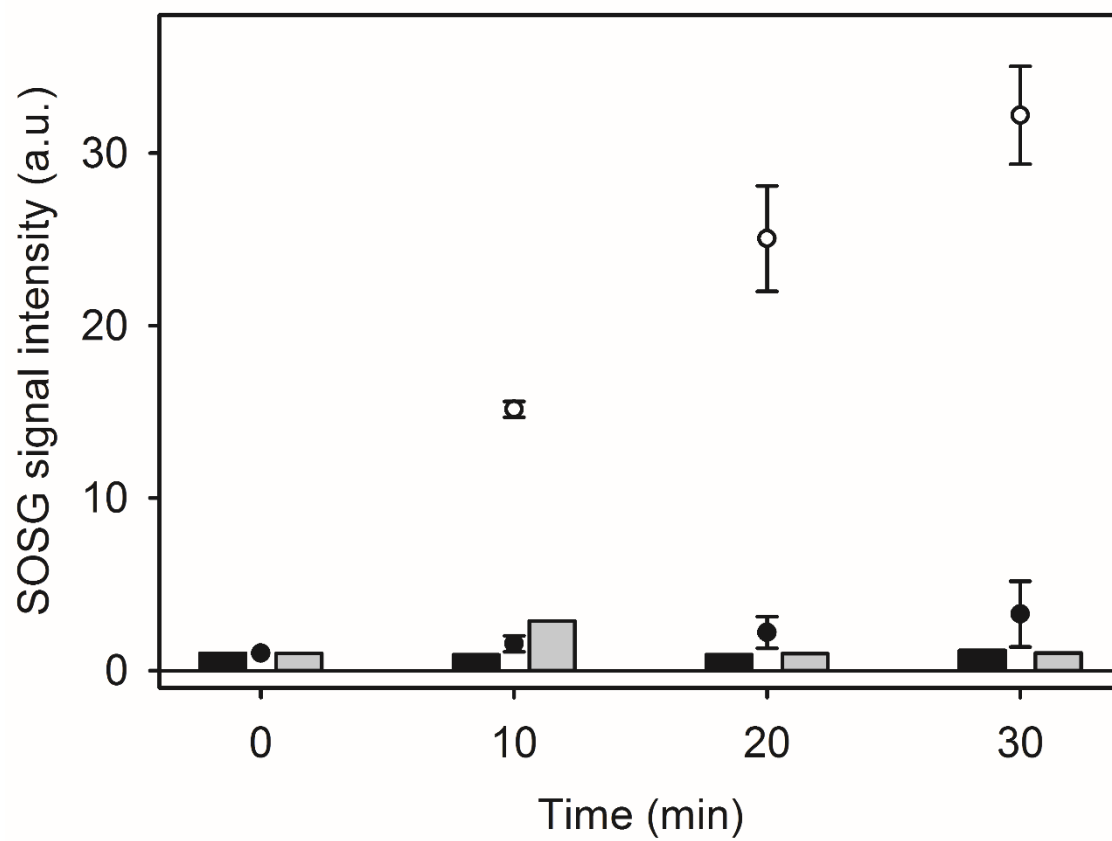
965



966

967 **Fig. 6.**

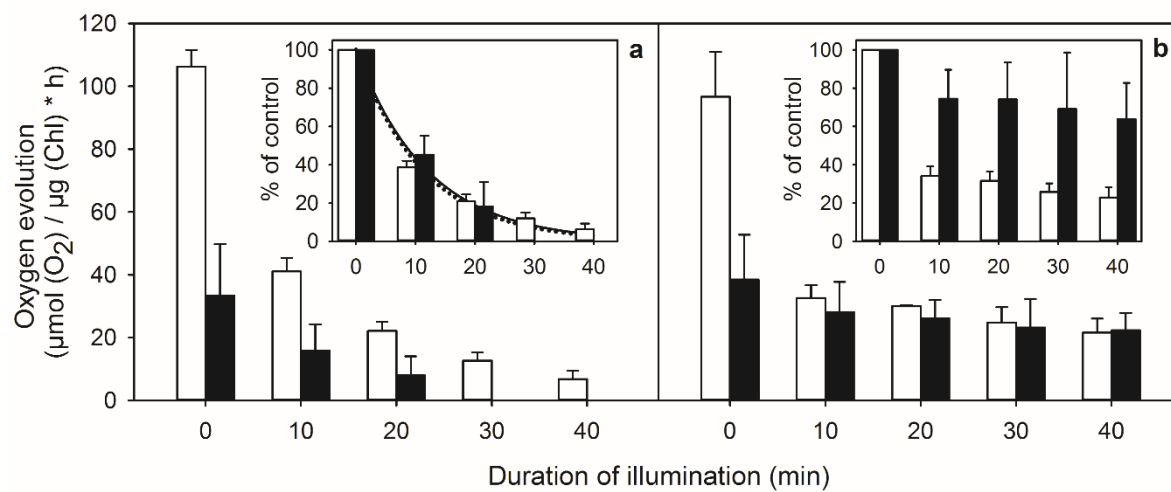
968



969

970 **Fig. 7.**

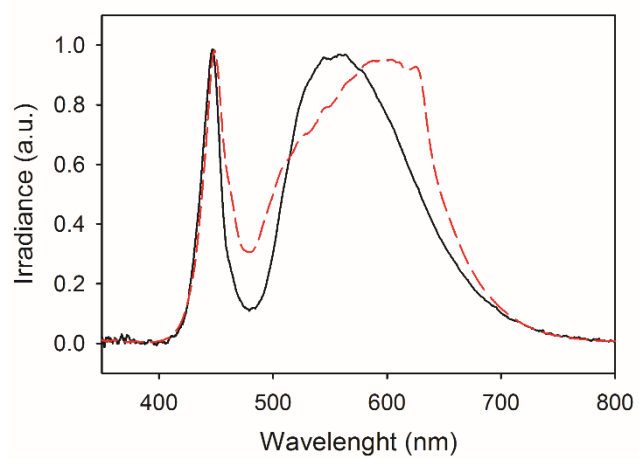
971



972

973 **Fig. 8.**

974

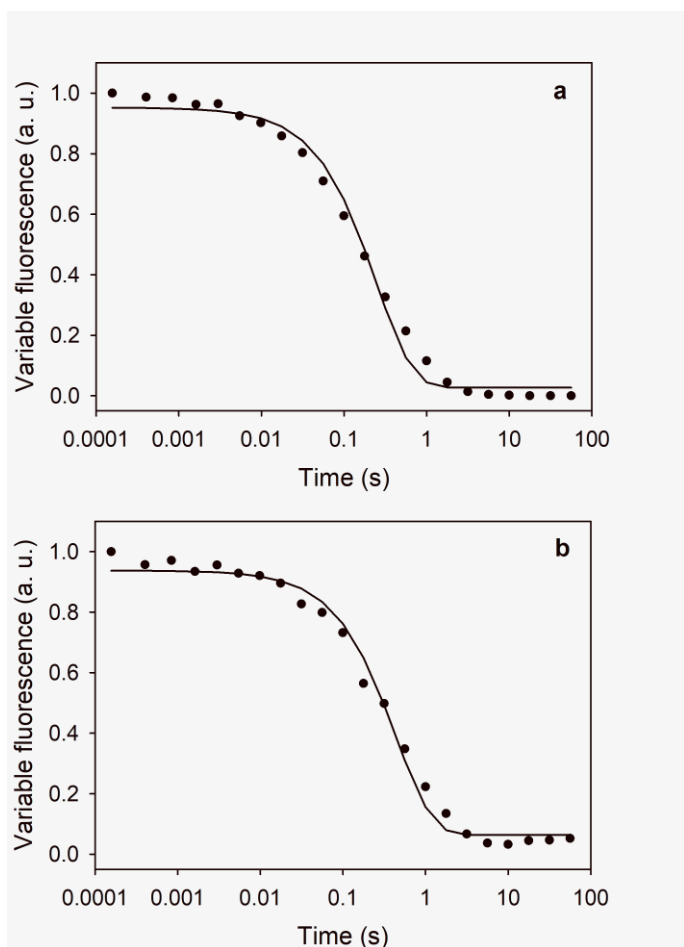


975

976 **Fig. S1**

977

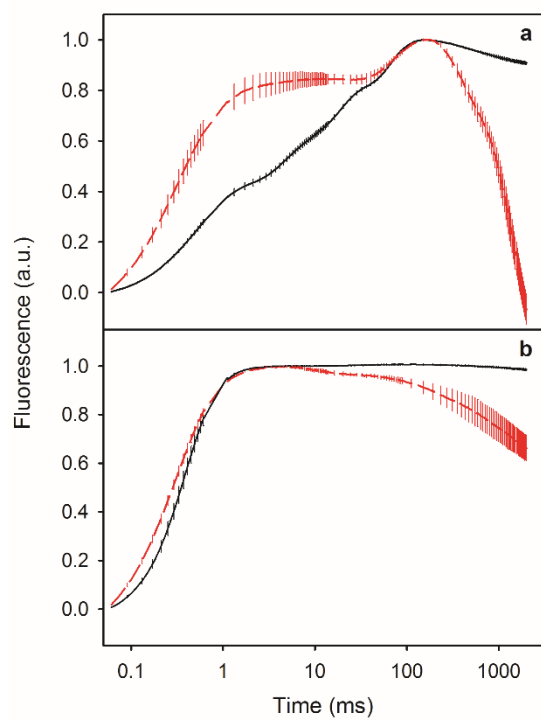
978



979

980 **Fig. S2**

981



982

983 **Fig. S3**

984

985

